Journal of Management Science & Engineering Research

Editor-in-Chief

Seyed Ehsan Hosseini   Arkansas Tech University, United States

Editorial Board Members

Journal of Management Science & Engineering Research

Editor-in-Chief

Seyed Ehsan Hosseini

Contents

Article

Review

Copyright

Journal of Management Science & Engineering Research

http://ojs.bilpublishing.com/index.php/jmser

ARTICLE

An Advanced Simple Method for Generating Synthetic Average Instant Hourly Solar Energy

Can Coskun*   Zuhal Oktay

Mechanical Engineering Department, Faculty of Engineering, İzmir Democracy University, İzmir, 35800, Turkey

ABSTRACT

The main objective of this study is to generate accurate synthetic hourly solar radiation data by using an easily accessible open source data. In this regard, a new approach is proposed for estimation of synthetic hourly global solar radiation during the day by utilizing only annual solar energy data. First time in literature, a model has been developed for prediction hourly and daily solar radiation based on annual solar energy parameter in this study. Parameters of the model were generated and tested for Turkey and one of them was presented as a case study within this paper. Long term measured hourly horizontal solar irradiance data from a network of Turkish meteorological stations was used to calibrate the model function. The predictions are compared with the solar data available in literature for Turkey. The advanced simple new model is utilized in open source computer program and has the potential to be adapted to other countries.

1.Introduction

The increasing use of solar power as a source of electricity has led to increased interest in forecasting short time solar radiation. Forecasted short time solar radiation data is generally used for simulation of the solar power plants such as photovoltaic and concentrated solar power systems.[1,2] The hourly solar-radiation amount is one of the important parameters for design and efficient operation of solar-energy systems. Forecasting short time solar radiation is neither completely random nor deterministic. It is necessary to know the possible short time trend of weather data such as solar radiation, outdoor temperature and wind speed for solar power plant simulations of energy and economics.[3] In this respect, many researchers have focused on new models to generate synthetic hourly data. Laslett et al.[2] developed an algo-

rithm to generate synthetic hourly cloudiness data for any time of the year at any location in the southwest region of Western Australia (WA). In their study, hourly cloudiness data was generated from the daily values using a first order autoregression algorithm with time varying mean and standard deviation. Yang and Koike[4] developed a numerical model to estimate global solar irradiance from upper-air humidity. In their study, a sky clearness indicator was parameterized from relative humidity profiles. Numerical model was tested at 18 sites in Japan, and hence the relationship between global solar radiation and sky clearness indicator was investigated. They found that global solar radiation strongly depends on the sky clearness indicator. Gordon Reikard[1] compared the Autoregressive Integrated Moving Average (ARIMA), Unobserved Components models, transfer functions, neural networks, and

Corresponding Author:
Can Coskun,
Mechanical Engineering Department, Faculty of Engineering, İzmir Democracy University, İzmir, 35800, Turkey;
E-mail: can.coskun@idu.edu.tr.

hybrid models to predict solar radiation at high resolution. He noticed that the best results are obtained using the ARIMA in logs, with time-varying coefficients. Chandel and Aggarwal[5] tested two models for estimation of hourly solar radiation in Western Himalayas. Many individual studies[6-9] have been carried out in recent years on testing current models for different locations of the world. Determination of the model parameters for each province is the main limitation of the synthetic hourly solar energy determination models. There is calculation model in open literature which is collecting model parameters in a simple formulation for a country. Fouilloy et. al.[10] analyzed the eleven statistical and machine learning tools tor forecasting the hourly solar irradiation. The most efficient models are determined. Anand et al.[11] tested some existing solar radiation prediction models. They compared the measured data and selected models. They proposed a new model in open literature. Ngoko et al. [12] presented a model for the synthetic generation of 1-min global solar radiation data starting from the daily clearness index. They tested the statistical characteristics of the measured and synthetic data sets.

The web page-based Solar-Med-Atlas program (URL 1) and PVGIS photovoltaic software (URL 2) are important simulation programs that predict solar energy potential and PV electricity production for many locations in the Word. These programs allow us to calculate the total energy amount per month or year. Also, there is no option to calculate the hourly synthetic solar energy amount for any chosen day. This study contributes to researchers, practitioners and energy investors to calculate the hourly probable average global solar radiation amount in a practical way by using one formulation. Researchers can utilize the formulation procedure or given formulation to write computer program about the determination of hourly solar energy amount and PV electricity production for Turkey. Synthetic average instant global solar radiation is important parameter for determination of the surface temperature of the PV systems[13]. In the present study, an advanced simple method for simulating hourly global solar radiation was developed and implemented for Turkey. Many models proposed to literature for the prediction of solar radiation are utilized existing climatic-parameters, such as cloud cover, sunshine duration, relative humidity and outdoor temperatures[14-23]. Controversially, first time in literature, a model has been developed for prediction hourly and daily solar radiation based on total annual global solar radiation parameter in this study.

To show the reliability of the model, the results are compared with the solar data available in literature for Turkey.

2. The Detrend Models for Hourly Solar Radiation

Some models that model the general distribution of hourly solar series:

2.1. Jain's Model

Jain's model[24] utilizes a Gaussian function for the solar radiation series. Model function is given below:

$$r_h = \frac{1}{\sigma\sqrt{2\pi}} exp\left[-\frac{(h-m)^2}{2\sigma^2}\right]$$

r_h and h indicates the solar radiation and time. σ is the standard deviation of the Gaussian curve. The parameter m represents the peak hour of a day.

2.2. Baig's Model

Baig's model[25] modified the Jain's model to get better accuracy at the start and end of series. Baig's model is:

$$r_h = \frac{1}{\sigma\sqrt{2\pi}}\left\{exp\left[-\frac{(h-m)^2}{2\sigma^2}\right] + \cos\left(180\frac{(h-m)^2}{S_0-1}\right)\right\}$$

s_0 is the sunshine hour of the day at a site with latitude φ and sun's declination could be calculated by:

$$S_0 = \frac{2}{15}\cos^{-1}(-tan\varphi \cdot tan\delta)$$

δ is the angle between the rays of the Sun and the plane of the Earth's equator.

2.3. S. Kaplanis' Model

Kaplanis[26] proposes a sinusoidal function for the solar radiation series.
That is:

$$r_h = a + b \cdot \cos\left(\frac{2\pi(h-m)}{24}\right)$$

a and b in the equation are the model parameters. m is the peak hour of solar radiation.

2.4. Al-Sadah's Model

Al-Sadah[24] proposes a polynomial model in fitting hourly global radiation on a horizontal surface.
$r_h = a_1 + a_2 h + a_3 h^2$

3. New Model for Synthetic Average Instant Global Solar Radiation

The starting point of this study is the given question; Is there any relation between annual solar energy amount and hourly average solar radiation trend? In this perspective, hourly global solar radiation data taken from Turkish meteorological data stations in Turkey were analyzed. Turkey is divided into 40 regions from 1200 W / m² year

to 2000 W / m^2 year with 20 W step. Changing between 19 and 40 years of total solar radiation data were analyzed. Nearly 500 000 hours of data are considered for the advanced model parameters. First of all, model parameters (a, b, c, d) are determined for each day from the first day of December. 365 function was calculated for each region. Total 14600 different functions (365 days x 40 regions) Computer program was written in python computer program. Then each model parameter of each day for 40 regions was taken to another calculation procedure. New 365 functions were determined for each day. The hourly average global radiation function was adopted to Gaussian function based on annual solar energy similar to Jain's model. End of the calculation procedure 365 functions were collected to one function. Flow diagram of the model parameters calculation procedure is given in Fig. 1.
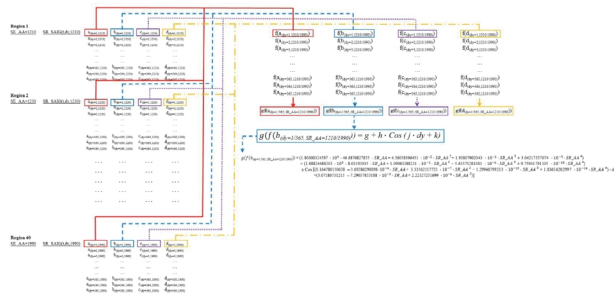

Figure 1. Flow diagram of the model parameters calculation procedure

Average global solar radiation change during the day for each location in Turkey is formulated according to time and day. The synthetic average instant global solar radiation of any time on a horizontal surface (*SR_SAIG*) in kW/m^2 can be estimated using the following equation;

$$SR\_SAIG(t, dy, SR\_AA) = a \cdot b \cdot exp\left[\frac{-(t-c)^2}{2 \cdot d^2}\right] \tag{1}$$

In Equation (1), *dy* is the number of the day with count starting on January 1st. While the first day of January is *dy* = 1, for the last day of December this value is 365 in the formula. *t* indicates hour of the day. SE_AA is actual annual solar energy amount in kWh/m^{2}year. Model parameters for Turkey are determined for 1200 to 2000 kWh/m^{2}year, annual solar energy limits. The parameter to 'a' is the correction factor depending on the error rate. The parameter to 'b' represents the peak solar energy of a day. The parameter to *c* represents the peak hour of a day. The parameter to 'd' is related to slope of the function. In Equation 1, a, b, c, d are the model parameters for Turkey and can be found by the equations below:

$$a = -6.47255533646 + 2.64499284473 \cdot 10^{-2} \cdot SR_{AA} - 3.68859978191 \cdot 10^{-5} \cdot SR_{AA2} + 2.53327237263 \cdot 10^{-8} \cdot SR_{AA}{}^3 - 8.56828030062 \cdot 10^{-12} \cdot SR_{AA}{}^4 + 1.14215701185 \cdot 10^{-15} \cdot SR_{AA} \tag{2}$$

$$b = g + h \cdot Cos(j \cdot dy + k) \tag{3}$$

$$g = 1.80300324597 \cdot 10^4 - 46.6876827855 \cdot SR_{AA} + 4.56058396451 \cdot 10^{-2} \cdot SR_{AA}{}^2 - 1.93807902043 \cdot 10_{-5} \cdot SR_{AA}{}^3 + 3.04217557074 \cdot 10^{-9} \cdot SR_{AA}{}^4 \tag{4}$$

$$h = 1.68824486203 \cdot 10^3 - 8.03193915952 \cdot SR_{AA} + 1.09963388231 \cdot 10^{-2} \cdot SR_{AA}{}^2 - 5.61575281081 \cdot 10^{-6} \cdot SR_{AA}{}^3 + 9.75941791105 \cdot 10^{-10} \cdot SR_{AA}{}^4 \tag{5}$$

$$j = 0.164780150638 - 3.69286290098 \cdot 10^{-4}) \cdot SR_{AA} + 3.33562517725 \cdot 10^{-7} \cdot SR_{AA}{}^2 - 1.29948799213 \cdot 10^{-10} \cdot SR_{AA}{}^3 + 1.83616202997 \cdot 10^{-14} \cdot SR_{AA}{}^4 \tag{6}$$

$$k = 3.07186731215 - 7.29057853188 \cdot 10^{-3} \cdot SR_{AA} + 2.22327251699 \cdot 10^{-6} \cdot SR_{AA}{}^2 \tag{7}$$

$$c = 12.6921252445 + 0.21148171825 \cdot Cos(0.0207537604614 \cdot dy - 3.73567688657) \tag{8}$$

$$d = l + m \cdot Cos(n \cdot dy + p) \tag{9}$$

$$g = -42.3695859121 + 0.121453134826 \cdot SR_{AA} - 1.21712391834 \cdot 10^{-4} \cdot SR_{AA}{}^2 + 5.33992381107 \cdot 10^{-8} \cdot SR_{AA}{}^3 - 8.63315621218 \cdot 10^{-12} \cdot SR_{AA}{}^4 \tag{10}$$

$$m = -26.8947926096 + 7.27191943559 \cdot 10^{-2} \cdot SR_{AA} - 7.15213685864 \cdot 10^{-5} \cdot SR_{AA}{}^2 + 3.07986310837 \cdot 10^{-8} \cdot SR_{AA}{}^3 - 4.88955117317 \cdot 10^{-12} \cdot SR_{AA}{}^4 \tag{11}$$

$$n = 0.555251443826 - 1.40928564028 \cdot 10^{-3} \cdot SR_{AA} + 1.36740867243 \cdot 10^{-6} \cdot SR_{AA}{}^2 - 5.81017686505 \cdot 10^{-10}) \cdot SR_{AA}{}^3 + 9.10938734424 \cdot 10^{-14} \cdot SR_{AA}{}^4 \tag{12}$$

$$p = -112.6409927302 + 0.281627123207 \cdot SR_{AA} - 2.67400324374 \cdot 10^{-4} \cdot SR_{AA}{}^2 + 1.11034109891 \cdot 10^{-7}) \cdot SR_{AA}{}^3 - 1.6998037957 \cdot 10^{-11} \cdot SR_{AA}{}^4 \tag{13}$$

In order to run the proposed model, the annual solar energy amount should be used. Three main parameters, namely the annual solar energy amount, time and day, are then employed to simplify the approach. The average total annual solar radiation amount for each province is provided in different web site such as Turkish State Meteorological Service's web sites. The synthetic daily average solar energy (SE_SAD) in kWh/m^2 can be estimated using the following equation;

$$SE\_SAD(t) = \int_5^{21} SR\_SIG(t) \cdot dt$$
$$= \int_5^{21} a \cdot b$$
$$\cdot exp\left(\frac{-(t-c)^2}{2 \cdot d^2}\right) \cdot dt \tag{14}$$

As can be seen from Equation 14, synthetic daily average solar energy can be estimated by the summation of hourly solar radiation between 05:00 and 21:00. Synthetic daily average solar energy trend is calculated and given in Fig. 2 between 1300 and 2000 kWh/m^2 year. As can be seen from Fig. 2, the synthetic daily average solar energy for Turkey varies between 1 and 8 kWh/m^2 day during the year. Annual total global solar radiation map for Turkey is given in Fig. 3. Effect of model parameters for synthetic average instant global solar radiation variation during the year is shown in Fig. 4.
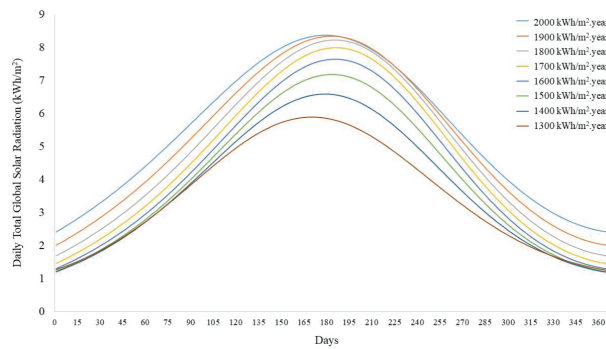
Figure 2. Daily total global solar radiation variation between 1300 and 2000 kWh/m^2 year
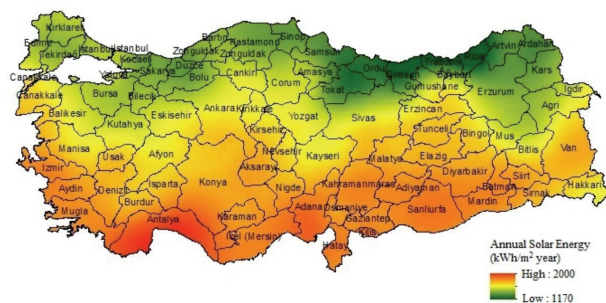
Figure 3. Annual total global solar radiation for Turkey
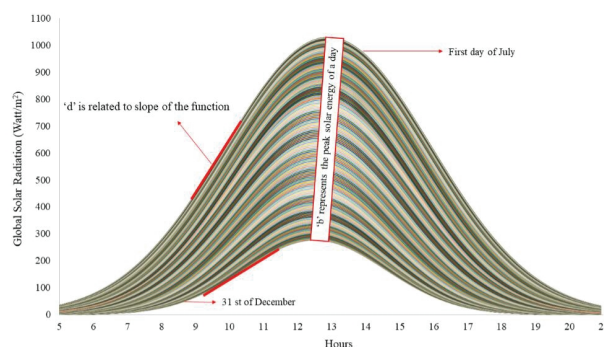
Figure 4. Synthetic average instant global solar radiation variation

Errors rate analysis was performed using the method described by Holman [25].

$$um\ Error(x_n)$$
$$= \sqrt{Error(x_1)^2 + Error(x_2)^2 + \cdots + Error(x_n)^2}$$

$$\bar{x} = \frac{Sum\ Error(x_n)}{n}$$

Here, n and is number of the test and average error rate, respectively. Average error rate was calculated for 81 providence and given in Fig. 5. The highest error rate amount is achieved in Ardahan and Ağrı. As can be seen from Fig. 4, users can determine the synthetic average instant global solar radiation during the chosen day. Annual and monthly solar energy results also compared to Solar-Med-Atlas program (URL 1) and PVGIS photovoltaic software (URL 2). Similar results are determined.
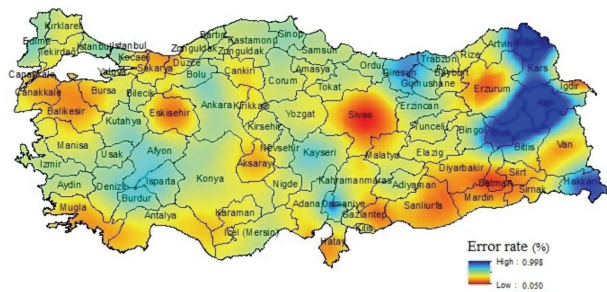
Figure 5. Map of the model error rate

4. Implementation of the Model for Turkey

The advanced simple method for synthetic average instant global solar radiation was implemented for Turkey. In order to illustrate the use of the present method, a case study was conducted for Beypazarı, Ankara in Turkey. The average annual solar energy amount (SE_AA) was 1450 kWh/m^2.year according to analyzed data.

The day and time is chosen as 15 of January and 12:00 In Equation 1, SE_AA, *dy* and *t* are 1450 kWh/m^2 year, 15 and 12, respectively. Synthetic instant global solar radiation (SR_SIG) is described as

$$SR\_SIG(t, dy, SR\_AA) = a \cdot b \cdot \left[2.71828^{\left(\frac{-(t-c)^2}{2 \cdot d^2} \right)} \right]$$

Model parameters were calculated by applying the Equation 1 to Equation 13 and given in Table 1.

Synthetic average instant global solar radiation for 12:00 can be guessed by applying the model parameters (a, b, c, d) as below

Table 1. Model parameters for 15 of January and 12:00 in Beypazarı

Parameters	Values(-)
a	1.001791
b	279.4
c	12.51446
d	2.033152
g	582.4
h	355.57
j	0.015633
k	-2.82504
l	2.4685
m	0.45355
n	0.01814
p	-3.12935

$SR\_SIG(12,15,1450)$

$= 1.001791 \cdot 279.4$

$\cdot \left[2.71828^{\left(\frac{-(12-12.48904)^2}{2 \cdot (2.033152)^2} \right)} \right]$

$_{January\ _{15}}^{12:00}SR\_SIG_{1450\ kWh/m2.year}$

$= 272\ Watt/m^2$

Synthetic average instant solar radiation value for 15 January is compared to actual yearly solar radiation data. The model generated synthetic average instantaneous solar radiation values with reasonably similar statistical characteristics to the measured data in Fig. 6.
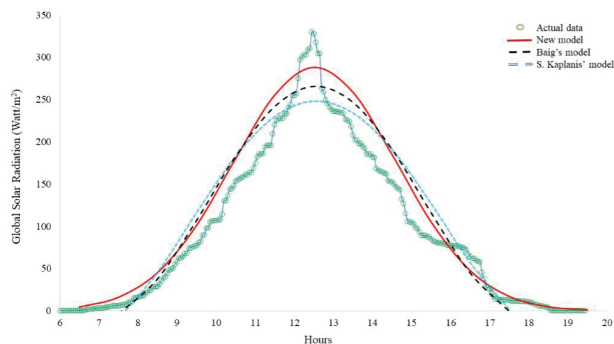
Figure 6. Comparison of new model to actual hourly data for 15 January

Screenshot photo of the written computer program in Pyton is given in Fig. 7. Solar energy amounts for any place of Turkey can easily determine any time range by utilizing written computer program.
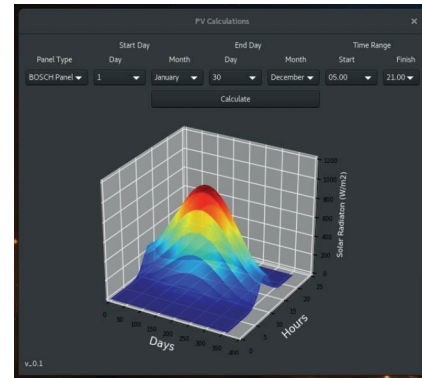
Figure 7. Synthetic average instant global solar radiation variation for Beypazarı during the year

5. Conclusion

The advanced simple method was designed to simulate solar irradiance on an hourly time scale for any location in Turkey. The results indicate that model can generate synthetic hourly horizontal radiation data with accuracies within the range of acceptable level. The comparison of the advanced simple method with the available data in the literature shows similar results. The model generated hourly solar radiation data with reasonably similar statistical characteristics to the measured data. New model has direct applicability for simulation of both thermal and PV concentrated solar power systems. Some findings of this study are as follows:

① Advanced simple method makes it possible to define the hourly solar radiation trend based on total solar radiation amount.

② A meaningful correlation was achieved between the variations of hourly solar radiation trend and annual solar energy amount in Turkey.

③ The advanced simple model is available in computer programs for solar energy calculations.

Future aim is to determine the model formulations for each county and adapted to other countries.

NOMENCLATURE

SR_AHAG	actual hourly average global solar radiation, kW/m^2
SR_ADAG	actual daily average global solar radiation, kW/m^2
SE_SAD	synthetic average daily solar energy, kWh/m^2
SE_AA	average annual solar energy, kWh/m^2year
SR_SAIG	synthetic average instant global solar radiation, kW/m^2
t	hour of the day.
dy	number of the day

Reference

[1] Reikard, G. Predicting solar radiation at high resolutions: A comparison of time series forecasts. Solar Energy 2009;83:342–49

[2] Laslett, D., Creagh, C., Jennings, P. A method for generating synthetic hourly solar radiationdata for any location in the south west of Western Australia, in a world wide web page. Renewable Energy 2014;68:87-102

[3] Knight, KM, Klein, SA, Duffie, JA. A methodology for the synthesis of hourly weather data. Solar Energy 1991;46(2):109–20

[4] Yang, K, Koike, T. Estimating surface solar radiation from upper-air humidity. Solar Energy 2002;72(2):177–86

[5] Chandel, S.S, Aggarwal, R.K. Estimation of Hourly Solar Radiation on Horizontal and Inclined Surfaces in Western Himalayas. Smart Grid and Renewable Energy 2011; 2:45-55

[6] Singh, O.P, Srivastava, S.K, Pandey, G.N. Estimation of hourly global solar radiation in the plane areas of Uttar Pradesh, India. Energy Conversion and Management 1997;38(8):779–85

[7] Parishwad, G.V., Bhardwaj, R.K, Nema, V.K. Estimation of hourly solar radiation for India. Renewable Energy Volume 1997;12(3):303-313

[8] Hussein, T.A.T. Estimation of Hourly Global Solar Radiation in Egypt Using Mathematical Model. Int. J Latest Trends Agr. Food Sci. 2012;2(2):74-82

[9] Yang, K, Koike, T. A. General model to estimate hourly and daily solar radiation for hydrological studies. Water Resources Research 2005;41(10): doi/10.1029/2005WR003976/full

[10] Fouilloy, A., Voyant, C., Notton, G., Motte, F., Paoli, C., Nivet, M.L., Guillot, E., Duchaud, J.L. 'Solar irradiation prediction with machine learning: Forecasting models selection method depending on weather variability', Energy, 2018;165;620-629

[11] Anand, M., Rajapakse, A. D., Bagen, B. Analysis of the Quality of Long-term Synthetic Solar Radiation Data Generated from Stochastic Models, 2018 IEEE International Conference on Probabilistic Methods Applied to Power Systems (PMAPS), Boise, ID, 2018, pp. 1-6. doi: 10.1109/PMAPS.2018.8440560

[12] Ngoko, B.O., Sugihara, H., Funaki, T. Synthetic generation of high temporal resolution solar radiation data using Markov models. Solar Energy, 2014;103:160-170

[13] Coskun, C., Toygar, U., Sarpdag, O., Oktay, Z. Sensitivity analysis of implicit correlations for photovoltaic module temperature: A review(Review). Journal of Cleaner Production 2017;164:1474-1485

[14] Badescu, V. Correlations to estimate monthly mean daily solar global-irradiation: application to Romania. Energy 1999;24(10):883–93

[15] Ecevit, A, Akinoglu, B.G, Aksoy, B. Generation of a typical meteorological year using sunshine-duration data. Energy 2002;27(10):947–54.

[16] Coskun, C., Oktay, Z., Dincer, I. Estimation of Monthly Solar Radiation Intensity Distribution for Solar Energy System Analysis. Energy 2011;36 (2):1319-1323

[17] Akyuz, E., Coskun, C., Oktay, Z, Dincer, I. A novel approach for estimation of photovoltaic exergy efficiency. Energy 2012;44:1059–1066

[18] Oktay, Z., Coskun, C., Ertürk, M. Prediction of daily average global solar radiation and parabolic monthly irradiation model parameters for Turkey. Progress in Exergy, Energy, and the Environment, 2014;867-874

[19] Singh, O.P, Srivastava, S.K, Gaur, A. Empirical relationship to estimate global radiation from hours of sunshine. Energy Convers Management 1996;37(4):501–4

[20] Trabea, A.A, Shaltout, M.A. Correlation of global solar-radiation with meteorological parameters over Egypt. Renew Energy 2000;21(2):297–308

[21] Hepbaslı, A., Ulgen, K. Prediction of solar-radiation parameters through the clearness index for Izmir, Turkey. Energy Source 2002;24(8):773–85.

[22] Ulgen, K., Hepbaslı, A. Comparison of solar-radiation correlations for Izmir, Turkey. Int J Energy Res 2002;26(5):413–30

[23] Dincer, I, Dilmac, S., Ture, I.E, Edin, M. A. Simple technique for estimating solar-radiation parameters and its application to Gebze. Energy Conversion and Management 1996;37 (2):183–198

[24] Baig, A., Achter, P., Mufti, A. A novel approach to estimate the clear day global radiation. Renew Energy 1991;1: 119–123

[25] Bevington P.R, Data Reduction and Error Analysis for the Physical Sciences. MCGraw Hill Book Co., New York, 1969.

[26] Kaplanis S.N. New methodologies to estimate the hourly global solar radiation; comparisons with existing models. Renewable Energy 2006;31:781–790.

[27] Al-Sadah, F.H., Ragab, F.M., Arshad, M.K., Hourly solar radiation over Bahrain. Energy 1990;15(5):395-402

[28] Holman, J.P. . Analysis of experimental data J.P. Holman (Ed.), Experimental methods for engineers, McGraw Hill, Singapore (2001), pp. 48-143

URL 1. Solar-med-atlas. http://www.solar-med-atlas.org/solarmed-atlas/map.htm#t=ghi. (Accessed 16 January.2018)

URL 2. http://re.jrc.ec.europa.eu/pvgis/apps4/pvest.php (Accessed 16 January.2018)

ARTICLE

Chinese Journals' Chief Editors Should Enhance Their Response Rate to Authors

Jianjun Cao*   Xiaofang Zhang

College of Geography and Environmental Science, Northwest Normal University,Lanzhou 730070, China

ARTICLE INFO	ABSTRACT
	Chief editors are the souls of journals, and can guarantee a journal's success by enhancing the efficiency of the manuscript submission and publication process through promptness and speedy response rates to authors. In this study, a total of 867 international journals—indexed by Science Citation Index, Social Sciences Citation Index, and Arts & Humanities Citation Index, and 567 Chinese journals—indexed by Chinese Science Citation Database and Chinese Social Science Citation Information database, were randomly selected to explore whether significant differences in the response rate and speed exist between chief editors.639 chief editors' email addresses were obtained for the international journals, whereas 357 email addresses were gathered for the Chinese journals. However, due to mail servers, only 274 international and 330 Chinese editors were successfully contacted. All messages contained a questionnaire geared to determine the total length of time required for the manuscript submission and publication process. After two months, a 100% response rate was achieved for international chief editors, while Chinese chief editors had a significantly lower rate ($P < 0.01$) of 30.6%. Nevertheless, for both international and Chinese chief editors, 66% and 58% provided a response within 12 hours, respectively. Although several reasons exist for the Chinese journals' lagging behind international journals, this study demonstrates that the response rate of chief editors to authors may also be a contributing factor. Thus, chief editors of Chinese journals should enhance their response rate to improve the current situation and further contribute to Chinese journals' success.

1. Introduction

In recent years, China has allocated extensive human, material, and financial resources to scientific research[1]; however, despite substantial investments, only 148 of 6000 Chinese journals published in English were listed in the Journal Incitation Reports (JCR) published by Thomson Reuters. Furthermore, a limited number of these journals have achieved high international influence when compared to journals published in the United States (US) and United Kingdom (UK)[2-6].As a result, researchers are heavily inclined to publish their work in the latter international journals[7], particularly those indexed by Science Citation Index (SCI), Social Sciences Citation Index (SSCI), and Arts & Humanities Citation Index (A&HCI).

In addition to international exposure, researchers are further motivated to publish in international journals giv-

en: (*i*) their wish to strengthen academic exchanges and enhance international influences driven by academic internationalization; (*ii*) the promotional and reputational needs of Chinese universities (colleges) and research institutions as shaped by the range of impact of their publications; (*iii*) the lack of integration between disciplines which limits publication options and exposure for cross-disciplinary research; and (*iv*) the high fees charged for publication in Chinese journals which exceed many authors' ability to pay[8-14]. As a result, many researchers choose to incur the high international journal fees, despite potential low impact factors, to gain international recognition within their fields. Additionally, many international journals provide free publication, and have accordingly gained traction and attracted many authors. Moreover, the attitudes of editors, especially chief editors (CEs), also play an important role in attracting authors to a journal[15]. Therefore, it is essential to understand whether a difference exists between the attitudes of international and Chinese CEs, including response speed and rate, to provide effective recommendations to ensure journal success.

2. Research Methods

2.1 Selection of Journals

The international journals surveyed were drawn from the Science Citation Index (SCI), Social Sciences Citation Index (SSCI), and Arts & Humanities Citation Index (A&HCI) listed in 2015, whereas Chinese journals were garnered from the Chinese Science Citation Database (CSCD) and Chinese Social Science Citation Information (CSSCI) database. Given the large number of available international and Chinese journals, 10% and 33%, respectively, were selected using a random sampling method. Impact factors,

number of annual issues, and number of papers published of the journals selected are presented in Table 1. One-way analysis of variance (ANOVA) was applied to determine the statistically significant differences. The least-significant-difference (LSD) test was used to compare the means of variables when the results of ANOVA were significant at $P < 0.05$. The geographic distribution of the international journals selected for this study is presented in Fig. 1.

Figure 1. The distribution of journal(s) from selected countries

2.2 Collection of CE Response Data

Following the selection of journals, an email was sent to each respective CE with the following question: "How long does one manuscript take from submission to publication? ".The email periods allocated for international and

Table 1. Information of selected journals from three international databases and two Chinese databases

Database	International Journal				Chinese Journal		
	SCI	SSCI	A&HCI	Total	CSCD	CSSCI	Total
Total	3786	3125	1758	8669	1200	533	1733
Selected	379	312	176	867	393	174	567
Number of annual issues	10.6 a	5.3b	3.3c		8a	10b	
Mean	7.4A				8.8B		
Impact factor	3.31b	1.20a	0.62a		0.75a	0.85b	
Mean	2.30A				0.79B		
Annual papers	197b	54a	72a		223a	254b	
Mean	138A				235B		

Note: Lowercase letters indicate significant differences (*P*<0.05) in number of annual issues, impact factors, and annual papers of journals among the three international databases and two Chinese databases. Different capital letters symbolize significant differences (*P*<0.05) in measured variables between international journals and Chinese journals.

DOI: https://doi.org/10.30564/jmser.v1i1.74

Chinese CEs were between July 2nd–September 2nd, 2017 and June 14th–August 14th, 2017, respectively.

3. Results

The emails of 74% (639 out of 867) of international and 63% (357 out of 567) of Chinese journals were obtained by various channels; however, only 274 and 330 emails were sent successfully for international and Chinese journals, respectively. The remainder of emails experienced delivery failures identified through mailer-daemon notices. Nevertheless, the distribution for successful email delivery is represented in Fig. 2 below. For the successfully delivered emails, the international and Chinese journals had 100% and 30.6% response rate, respectively, indicating a significant difference between these two ($p < 0.01$). For emails to which CEs provided a response, the response time was determined (Table 2). Based on the responses received, 66.06% of international and 58.25% (no significant difference, $P > 0.05$) of Chinese CEs provided a response within 12 hours. After a 24-hour time period, the response rate for both international and Chinese CE sharply declined. Nonetheless, little difference was observed in the response speeds between international and Chinese journal CEs.

Table 2. Recorded time of response for emails sent to and received by chief editors of international and Chinese journals

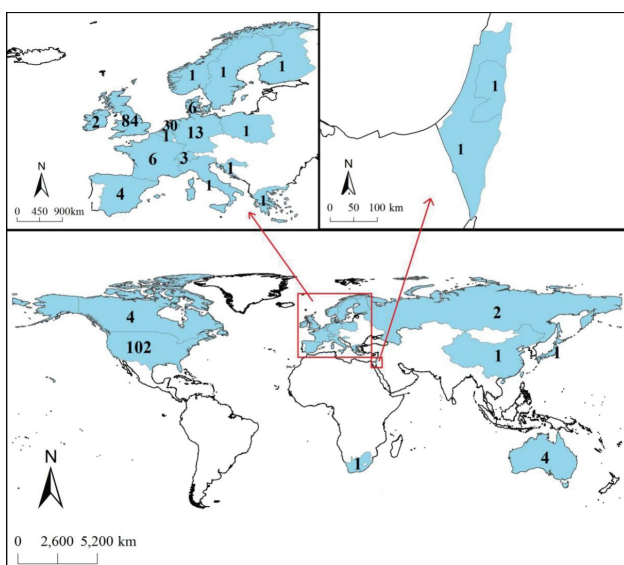| Type of chief editor	12 hours	24 hours	3-5days	6-10days	>10days
International journal	66.06	16.42	14.23	1.83	1.46
Chinese journal	58.25	28.16	9.70	2.91	0.98

Figure 2. Final distribution international journals having responded to the investigators' emails.

4. Discussion

Chinese journals lagged in terms of response rates when compared to international journals, especially those headquartered in the US and UK[4,6,8]. While this study presents a number of acceptable reasons for Chinese journals' limitations, it demonstrates that CEs' response to authors is a defining factor in the success of journals. The response rate for international CEs was significantly higher (approximately 70%) than Chinese CEs. Although other factors exist (shown in Table 1—impact factor, number of annual issues and annual papers) and are different between the two types of journals, statistical analysis indicated that these factors had no effect ($P > 0.05$) on email response rates. Therefore, in this case, CEs' individual behavior becomes a determinant factor for the rate of response to authors.

As an academic leader and steward, CEs bear an important role which includes building a journal's reputation through independent efforts[16,17]. These efforts include common responsibilities such as communication with authors, evaluation of manuscripts, manuscript review and communication with reviewers[16,18]. However, no supervision exists to ensure that the manuscript submission and publication process is efficient. The work is therefore dependent on the enthusiasm and motivation level the CE has for the work performed. For this reason, and based on the data collected, it could be stated that international journal CEs are more devoted to their role than CEs for Chinese journals. Furthermore, an additional reason for lower rates observed for the Chinese journals can be attributed to the fact that communication can be achieved directly by phone. This results in a lack of effective email communication driven by numerous Chinese journal CEs ignoring or taking emails for granted.

Nonetheless, although low response rates from Chinese CEs were determined, the response time (within 5 days) for the two types of journals was similar, suggesting equal enthusiasm from those whom responded. Therefore, if response promptness is maintained, the quality of the Chinese journal could greatly improve and guarantee success. In addition, the creation of new Chinese international journals could further attract authors in diverse fields. For example, in past decades, successful Chinese journals, such as Chinese Science Bulletin, Geography Journal, and Journal of Mountain Research, were internationalized through translation and the creation of English versions to reach a broader audience. This could be replicated with new journals as well.

5. Conclusion

CEs' response rate to authors of international journals

were significantly higher than those of Chinese journals; however, response speed between these two types of journals were found to be similar. The response rates of CEs were not related to publication factors of journals, but rather depended on CEs' individual behavior. CEs of Chinese journals should be aware that this limitation greatly contributes to the failures and successes of journals. Therefore, they should strengthen commitment to their responsibilities to ensure responses are provided to authors. As more open access journals are created by international publishers, Chinese journals must continue to develop and improve to remain competitive. For this reason, CEs must attract the better contribution sources as authors can be considered the "gods" of journals.

Acknowledgements

References

[1] Yao, S.J. Building a strong nation, how does China perform in science and technology. Asia Europe Journal,2006, 4(2), 197–209.

[2] Dong, X. and Zhang, S.Q., The Statistical Analysis of the Influence of Chinese Mathematical Journals Cited by Journal Citation Reports, Cross-Cultural Communication, 2015, 11(9), 24–28.

[3] Ding, Z.Q., Zheng, X.N. and Wu, X.M. Strategies for Expanding the International Influences of Academic Journals: An Example from Chinese Pharmaceutical Journals, Serials Review, 2012, 38(2), 80–85.

[4] Jia, X. The past, present and future of scientific and technical journals of China, Learned Publishing, 2006, 19(2), 133–141.

[5] Yang, Z.G., Feng, G. and Zhang, C.T. Comparison of Journal Self-Citation Rates between Some Chinese and Non-Chinese International Journals, Plos One, 2012, 7(11), e49001.

[6] Yang, S.L., Yuan, Q. L. and Han, L., Comparative Study of Papers' Impact in Open Access Journal Between China and the USA, Journal of Library Science in China, 2017, 43(1), 67–88. (in Chinese).

[7] Shao, J.F. and Shen, H.Y. (2011), The outflow of academic papers from China: Why is it happening and can it be stemmed? Learned Publishing, 2011, 24(2), 95–97.

[8] Ren, S.L. and Rousseau, R. International visibility of Chinese scientific journals, Scientometrics, 2002, 53(3), 389–405.

[9] Ren, S.L. and Rousseau, R. The role of China s English-language scientific journals in scientific communication, Learned Publishing,2004, 17(2), 99–104.

[10] Zhang, Y.H., Yuan, Y.C. and Jiang, Y.F. An international peer-review system for a Chinese scientific journal, Learned Publishing,2003, 16(2), 91–94.

[11] Zhang, F.L. and Li, L. Improving the International Influence of Chinese Academic Journals, Journal of Scholarly Publishing,2003, 34(2), 101–107.

[12] Wang, S.H. and Weldon, P.R. Chinese academic journals: quality, issues and solutions, Learned Publishing, 2006, 19(2), 97–105.

[13] Ge, J.P., Fan, Z.Z., Li M.M. and Cai, F. Some thoughts about the language internationalization of China's English-language sci-tech journals, Acta Editologica, 2013, 25(1), 48–50. (in Chinese).

[14] Xu, P., Yan H., Xiang L., Li, R.H. and Li, F. Discussion on the practice of international peer-review for English science and technology journals published in China: Taking Plasma Science and Technology as an example, Chinese Journal of Scientific & Technical Periodicals, 2017, 28(4), 312–319. (in Chinese).

[15] Besancenot, D., Faria, J. R. and Huynh, K.V. Search and Research: The influence of editorial boards on journals' quality, Theory & Decision,2012, 73(4), 687–702.

[16] Bogdanović, G. Publication ethics: The editor-author relationship, Archive of Oncology, 2003, 11(3), 213–215.

[17] Akhtar, J. Role of the editors in improving quality of medical journals, Journal of the Liaquat University of Medical & Health Sciences, 2012, 11(2), 52–53.

[18] Grammaticos, P. Editor and authors' psychology and the chance of teaching, Hellenic Journal of Nuclear Medicine, 2006, 9(3), 154–155.

REVIEW

Prediction of Formation Pressure Gradients of NC98 Field-Sirte Basin-Libya

Ahmed Tunnish[1]*   Mohammed Nasr[2]   Mahmoud Salem[3]

1. Petroleum Systems Engineering Department, Faculty of Engineering, University of Regina, Canada.

2. Petroleum Engineering Department, Faculty of Engineering, Tripoli University, Tripoli, Libya

3. Waha Oil Company, Tripoli, Libya.

ARTICLE INFO	ABSTRACT
	The prediction of formation pore pressure and fracture pressure gradients is a significant step towards the drilling plan. In this study, the formation pressures of twelve wells from NC98 field-Sirte Basin (Waha Oil Company) were calculated by employing empirical methods, Eaton's equations, that depend on the real drilling and well-logging data. Regarding the results, the normal pore pressure in the NC98 field in Sirte basin is 9.89 kPa/m (0.437 Psi/ft), and it is extending from the top of the wells in the investigated area to 2134 m (7,000 ft). A subnormal to normal pore pressure zone is noticed in the interval of 2134 m to 2743 m (7,000 ft. - 9,000 ft). Then, slightly subnormal to somewhat abnormal (overpressure) region is seen from 2743 – 3414 (9,000 ft. - 11,200 ft). Beyond to that depth and down to the top of the reservoir, the overpressure zone was clearly observed. Based on the results, the casing seating depth and the equivalent mud weight were simply determined for the area of study.

1. Introduction

One of the most significant factors for drilling preparation is the formation pore pressure. The pressure formed in pore spaces due to the presence of the fluids is known as formation pore pressure. Pore pressure is classified as subnormal (less than hy-drostatic pressure "9.8 kPa/m or 0.433 psi/ft"), normal (equal to hydrostatic pressure), and overpressure (slightly more than hydrostatic pressure and less than overburden pressure). Thermal expansion, under compaction, mineral transformations, hydrocarbon generation,..., etc. are some of the reasons for having formation pore overpressure

Corresponding Author:

Ahmed Tunnish

Petroleum Systems Engineering, Faculty of Engineering and Applied Science, University of Regina, Regina, Canada

E-mail: tunnisha@uregina.ca

zones. The abnormal compaction results in disequilibrium compaction, which concludes with the changing trend of the overburden pressure (probably decreasing) with the depth, more pore spaces, and overpressure[1]. Where the rapid sedimentation process and the presence of a no permeable system are the main reasons for creating overpressure zone[2]. The ratio of the pore volume of the formation decreases with depth in the case of regular compacted or pressurized zones[3]. Finally, the precise prediction of formation pore pressure is crucial to prevent drilling well blowouts, pressure kicks, and fluid influx.

Accurate prediction of formation pressures can benefit even the geologists historically to analyze the migration of the fluids from the mother rock (source rock) to the trap[4]. The precise prediction of the overpressure zone can be proved by the alteration in the overburden pressure gradient curve. According to the results, the predicted pore pressure is inversely related to the overburden pressure and linearly related to the fracture pressure; however, fracture pressure is straightly linked with both of them. Also, it was noticed that the overburden pressure mainly affected by the depth of the formation. Where it is directly proportional to the depth[5]. In the Gulf of Mexico, about 24 % of the drilling processes were ended up with loss circulation and flowing of water/gas, due to the wrong pre-drilling data[6].

The common methods to predict the formation pressures depend on pre-drilling information (seismic data), during drilling information (well-logging/drilling data), and history information (known data data)[7]. For wildcat wells, only seismic data may be available. For the development wells, the prediction of the formation pressure gradients depends on the well-logging and drilling data in the investigated area. The prediction of formation pressures in complicated geological regions raises the uncertainty of the applied prediction models[8]. A long time ago, before the application of well-logging data to predict formation pore and fracture pressures, the characteristics of shale (mudrock) was employed. The predicted pressure from this technique represents pore pressure in shale. Alternatively, different ways included the centroid method introduced by Dickinson (1953)[9], Bowers (2001)[10] and the different models suggested by Yardley and Swarbrick (2000)[11] as well as Meng et al., (2011)[12] were employed.

In this study, Eaton's drilling and well logging methods are employed to predict formation pore pressure and fracture pressure gradients for NC98 field-Waha-Sirte Basin. The predicted formation pressure gradients were applied to determine the equivalent mud circulation, casing seating depths, and the number of required casings in this area. Besides, figuring out the most appropriate source of

data (drilling or well logging data) that can be used to predict pore and fracture pressure gradients.

The goals of this study are: (1) studying the applicability of Eaton's methods in the studied area, (2) determining of the proper source of data (well logging or drilling raw data) to predict formation pressure gradients, (3) predicting the minimum and maximum pore pressure, and fracture pressure gradients and (4) establishing one plot of the collective formation pressure results for the future development projects in this area.

2. Description and Geology of NC98 Field-Waha-Sirte Basing:

NC98 is one of Waha Oil Company fields that are located in the southeastern section of Sirte basin that is found in the north-central part of Libya[13]. Sirte basin is the newest developed basin in Libya with the largest petroleum reserve. The producible quantity of the hydrocarbon in this basin is estimated at 45 billion Bbl of oil and 33 trillion ft3 of gas. Geologically, the source rocks of the Sirte basin are Upper Cretaceous Rachmat and Sirte shale rocks and reservoir formations are formed in Cretaceous and Eocene to Miocene rift structures age. Structurally, 58 % of the reservoirs are sandstone rocks (clastic), and the rest are carbonates rocks[14]. The lithology of Gialo - NC98 field is clearly shown in Fig. 1. The reservoir type is sandstone rock. The cap rock is mainly shale, salt mass, and claystone.
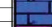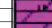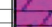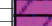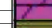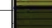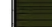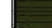
AGE		FORMATION	DEPTH (sub Sea ft)	LITHOLOGY	DESCRIPTION
Pleist-Plio		Loose sand			Loose sand, Clay
Miocene		Maradah			classic sediments, clay
					organic-rich shale
					Nubian quartzite's, Cenomanian dolomites,
			-1,550		Evaporates, fossils, anhydrites
Oligocene		Diba			Sandstone, shale, sandy limestone,
Eocene	Upper	Augila	-2,300		Shale sequence, argillaceous limestone
		El Erg	-2,700		Fossils, argilaceous and chalky
		Gialo	-2,900		Carbonates, argillaceous and chalky limestone
	Medium	Jakherrah	-3,530		Limestone, shale intervals, anhydrite, fossils
			-3,800		
		Al Gata			Dolomite, anhydrite, fossils
			-4,950		
	Lower	Gir			Dolomite, Anhydrite, chalky, fossils
Paleocene	Upper	Kheir	-5,850		Marlstone, claystone, micritic limestone
		U. Sabil	-7,250		Dolomite, Anhydrite
			-8,440		
	Lower	L. Sabil			Dolomite, Carbonates, shetrat shale
Cretaceous	Upper	Kalash	-9,640		Dense micritic limestone
		U. Sirte	-10,500		Shale, marlston
		Tagrfet	-10,750		Chalky carbonate, imbedded Shale carbonate,
		L. Sirte	-12,700		Shale, dolomite anhydrite, siltstone
		U. Salt	-13,350		Salt mass, Shale beds
		M C&A	-13,850		Dolomite, anhydrites, anhydrites mass
		L. Salt	-14,230		Salt mass, claystone
		T. Beds	-14,270		Shale, claystone, imbedded sandstone
Pre-U Cret		U. Nubian Sandstone	-14,418		Pay zone [Sandstone, quartz, claystone
		M. Shale MBR	-14,818		Claystone, imbedded w sandstone

Figure 1. The geology column of Gialo – NC98 (Waha Oil Company)[15]

3. Methods

This procedure is applied in the drilling application to predict formation pore pressure, fracture pressure and overburden pressure gradients for the formation. Monitoring the well-logging data, drilling data, drilling fluid, and rock particles, can be employed to indicate the transition zone between normal and overpressure areas.

3.1 Overburden Pressure Prediction

The precise prediction of formation pressures is essential in terms of the cost and safety during the drilling process. Overburden pressure can be determined based on the pore pressure data [16] by employing equation (1):

$$\sigma_{ob} = \sigma_v + \propto P_p \tag{1}$$

It is obvious from Equation (1) that the values of poroelasticity, vertical effective stress, and overburden pressure should be known to calculate formation pore pressure. The poroelasticity factor was experimentally proved as a constant ($\propto = 1$) by Terzaghi[17]. As can be noticed in Equation (2), in addition, the calculation of the overburden pressure mainly depends on the formation bulk density.

$$\sigma_{ob} = \int \rho_b \, dD \tag{2}$$

Gardner and coworkers (1974) found that the calculation of formation bulk density could be done through some empirical correlation based on seismic and well logging data[18]. Equation (3), as shown below, is directly employed to calculate the formation overburden pressure:

$$\sigma_{ob} = 0.433 \, \rho_b D \tag{3}$$

3.2 Pore Pressure Prediction

One of the important steps to prevent the possibility of having blowouts or mud loss during drilling step is the accurate prediction of formation pore pressure[2]. Since there is no straightforward method to measure formation pore pressure in some formations such as shales, planning, and execution of new boreholes depends on indirect ways[19]. Many methods such as Bowers[20], and d-exponent [21] are applied to predict the pore pressure in shales from indirect methods. The fundamental of the indirect techniques that are used to predict the abnormal pressure is based on the compaction of the studied formation. The abnormally pressured formations are less compacted and higher porous in comparison to formations of uniform lithology at the equivalent depth. So, formations with high porosity may be signified as overpressure areas. The indirect method proposed by Bingham (1969) depends on the hardness of the formation is known as the d-exponent method[22]. The d-exponent equation was modified based on drilling raw data to d-corrected-exponent (dc-exponent) to standardize the calculated drilling rate of penetration. Jorden's and Shirley's model was modified to include the

term of mud weight[23], as presented in equation (4):

$$dc - exponent = \frac{\log\left(\frac{ROP}{60\,RPM}\right)}{\log\left(\frac{12\,WOB}{10^3\,d_{bit}}\right)} * \left(\frac{\rho_{normal}}{\rho_{actual}}\right) \tag{4}$$

In 1975, Eaton proposed a predictive method of pore pressure depending on the drilling data (dc-exponent) and well logging (sonic compressional transit time) data, respectively, as presented in equations (5) and (6) [24]:

$$\frac{P_p}{D} = \frac{P_p}{D} - \left(\left(\sigma_{ob} - \frac{P_{pnormal}}{D}\right)\left(\frac{d_{c,observed}}{d_{c,normal}}\right)^{1.2}\right) \tag{5}$$

$$\frac{P_p}{D} = \frac{P_p}{D} - \left(\left(\sigma_{ob} - \frac{P_{pnormal}}{D}\right)\left(\frac{\Delta t_{normal}}{\Delta t}\right)^{3}\right) \tag{6}$$

3.3 Fracture Pressure Prediction

Formation fracture pressure (PF) is the pressure at which the formation starts cracking and the mud loss circulation occurs. For an appropriate mud weight design, it is crucial to accurately predict fracture pressure gradient. There are different methods to determine fracture gradient. In practice, fracture pressure is calculated from leak-off tests (LOT). From the literature review, the most popularly applied method is the Ben Eaton's fracture gradient prediction approach (Eaton 1975), as shown in equation (7). Yoshida et al. (1996) announced that Eaton's pore and fracture pressure gradient equations are applicable worldwide. This examination showed Eaton's fracture gradient prediction approach is one of the best techniques to use[19].

$$\frac{P_F}{D} = \frac{v}{1-v}\left(\frac{\sigma_{ob}}{D} - \frac{P_P}{D}\right) + \frac{P_P}{D} \tag{7}$$

The accurate prediction of overburden pressure gradient, pore pressure gradient and Poisson's ratio (Supplementary File-Poisson's Ratio calculation) of the studied area was essential to successfully apply Eaton's equation to calculate the fracture pressure gradient.

4. Results and Discussion

According to the combined dc-exponent results of the 12 investigated wells in the NC98 field, as shown in Fig. 2, we probably can say that the overpressure zone occurs. Where it starts with slightly decreasing in the dc-exponent data from 2,202 m to 3,048 m (7,223 ft - 10,000 ft), remarkably decreasing from 3,048 m to 3,658 m (10,000 ft to 12,000 ft), no deviation in the trend between 3,658 m and 4,572 m (12,000 ft and ~ 15,000 ft), and the data of dc-exponent is getting increased to the normal trend from 4,572 m to 4,952 m (15,000 ft - 16,250 ft). After that, the trend line reaches the equilibrium at the total depth (TD) 5,221.2 m (17,130 ft).
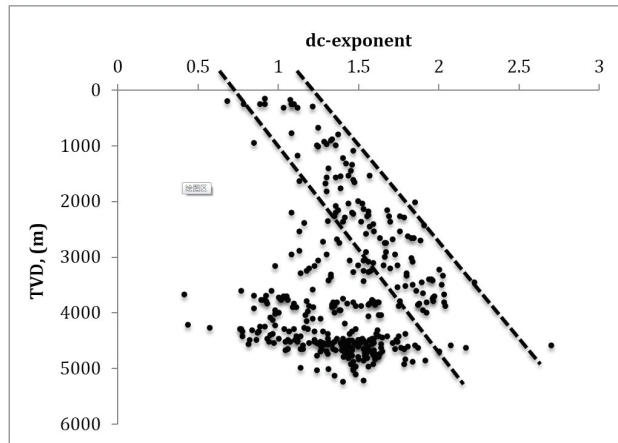
Figure 2. Modified dc-exponent values for the wells in the study area.

Similarly to dc-exponent, the deviation in the sonic log trend of one of the studied wells starts from 2,164 m (7,100 ft), which is increasing with depth, as can be seen in Fig. 3, opposite to the dc-exponent trend manner, which approves the presence of the overpressure zone. In details, the slight increasing begins from 2,164 m to 3,828 m (7,100 ft to 12,558 ft), notably increasing from 3,828 m to 4,797 m (12,558 ft - 15,738 ft), and the trend line is decreasing from 4,797 m to 4,907 m (15,738 - 16,100 ft). After that, the trend line is almost not changeable up to the Total Depth (TD). Up to now, drilling and logging data are matching and mostly approving the existence of the abnormal pressure (overpressure) zone.
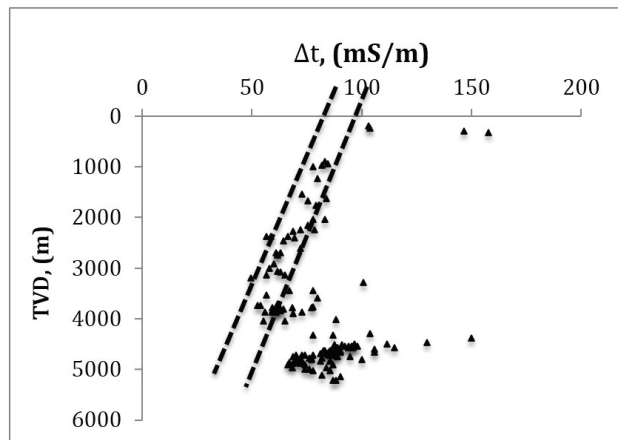

Figure 3. Sonic log records values for the wells in the study area.

The predicted pore pressure, fracture pressure, and overburden pressure gradients values from drilling raw data and well-logging records are presented in Fig. 4 and Fig. 5, respectively. Regarding the results, the overpressure zone can be clearly depicted from both drilling and logging source of data. The drilling data, as shown in Fig. 4, reveals that the normal pore pressure in the NC98 field at Sirte basin is 9.89 kPa/m, and it is extending from the top of the well to 2,134 m (7,000 ft). After that, subnormal to normal pore pressure zone was noticed in the interval of 2,134 m to 2,743 m (7,000 ft. - 9,000 ft). Then, the marginally subnormal to relatively abnormal (overpressure) zone was seen from 2,743 m to 3,414 m (9,000 ft. - 11,200 ft). At the cap rock, the overpressure zone was apparently detected. For the well-logging source of data, as represented in Fig. 5 for one of the studied wells in the area of study, almost similar results to the drilling data were observed from the top to 2,919 m (9,578 ft). Slightly subnormal to marginal overpressure zone was noticed from 2,919 m to 3592 m (9,578 ft - 11,786 ft). However, beyond that depth to 3,749 m (12,300 ft), it became impossible to differentiate between pore pressure and fracture pressure gradients, which will make it difficult to determine the casing seating depth and equivalent mud weight (EMW) for this region based on well-logging data. Once before, the formation pore pressure of NC202, Sirte basin was estimated by applying both Eaton's and Bowers Methods. It was found that the Bowers method was more accurate than the Eaton's method. Because Eaton's technique used in that study depended on the well-logging data, which is affected by the shale content and the shale content cannot typically be determined for the carbonate rock. The shale content does not influence the Bowers method, as it depends on the pre-drill data[25]. These outcomes agree with our results, as Eaton's drilling data formula concluded with better results than Eaton's well-logging method.

In general, the salt tectonics can change the formation compaction state, generating normal compaction pattern variations[7]. The abnormal compaction results with disequilibrium compaction, which concludes with the changing trend of the overburden pressure (probably decreasing) with the depth, more pore spaces, and overpressure[1]. Geologically, the subnormal to regular pore pressure interval in this area of study is mainly composed of Limestone, Chalky Limestone, Sandy Limestone, Dolomite, and evaporates. These formations are known with their total and effective porosity, which might be one of the reasons of having low to normal pore pressure area. However, the overpressure zone that is present in upper Sirte formation all the way down to lower salt formation T. beds (the cap rock) consists of shale and salt mass formations. These formations have high-disconnected porosity ratio that causes a noticeable increase in the pore pressure gradient. Proper prediction of pore and fracture gradient pressures is significant toward precise casing design[26]. Overall, the results of the dc-exponent, sonic log, formation logging,

and drilling pore and fracture pressures are matched, which confirms that we have a high-pressure zone in the abovementioned interval depth.
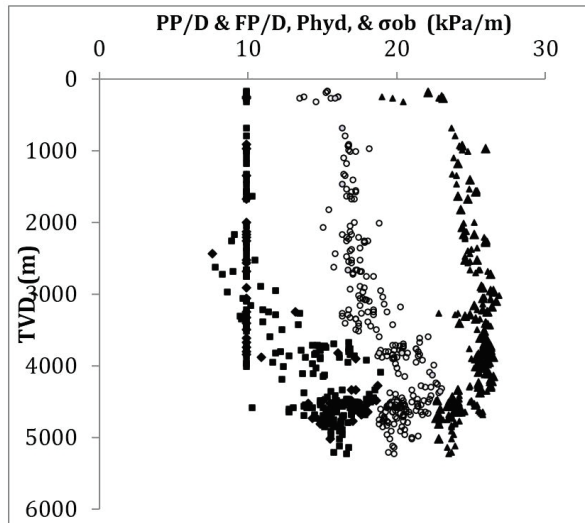
Figure 4. Predicted formation pressure gradients from drilling data
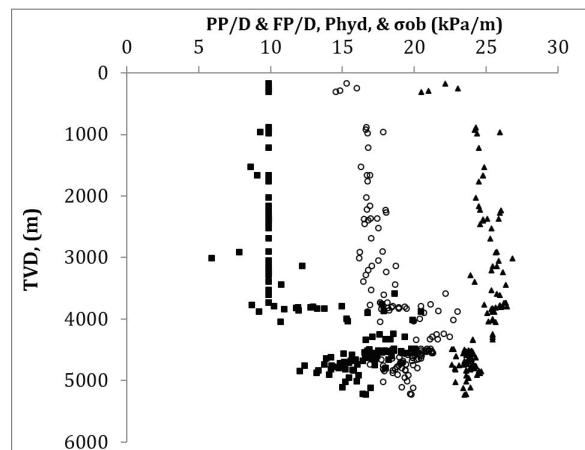
Figure 5. Predicted formation pressure gradients from well logging data

5. Casing Setting Depth

Besides formation pressure gradients, the seating depths and the number of casing strings also depend on geological conditions and the stability of freshwater aquifers. In deep wells, the principal concern is given to the control of abnormal pressure and of salt formations, which will tend to flow plastically[26]. The objective of placing the casing in the borehole is to inhibit the collapse while drilling. It is also employed to prevent the contact between the drilling fluids and formation fluid; reduce damage to the subsurface environment from the drilling operation and extreme subsurface conditions. Besides, it provides a great

strength and safe flow of the fluids through the well. In the determination of casing places, monitoring the maximum pore pressure and minimum fracture pressure gradients of the formation related to the depth of the studied area are needed, as shown in Fig. 6.
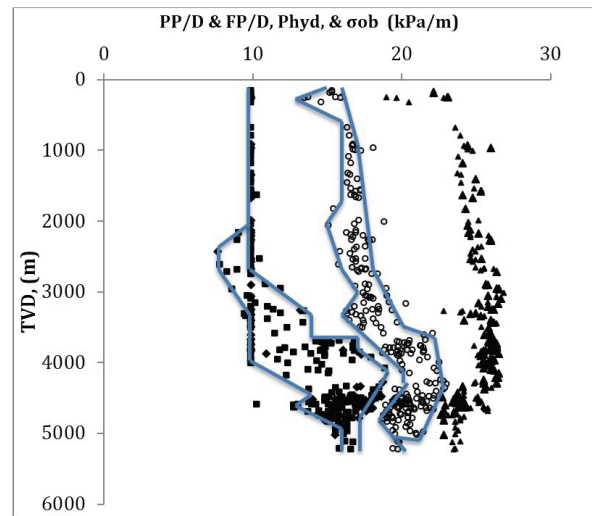
Figure 6. Estimating the minimum and maximum predicted formation pressure gradients from the drilling data

It is reasonable to employ the smallest fracture pressure trend line for casing depth design. After determining the minimum and maximum formation pressure gradients, the casing seating depth, the number of strings, and the EMW were easy to predict, as can be depicted from Fig. 7. Five casing strings are needed to prepare a casing design for this area. Besides, five mud weights are required to drill the wells appropriately in the studied field.
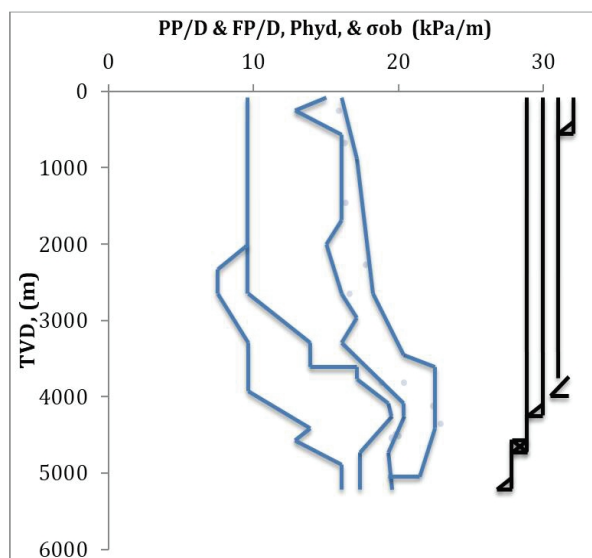
Figure 7. Estimating casing seating depths

Table 1. Predicted and actual mud weight and casing seating depths from drilling data

Casing #	Predicted Casing Depth	Predicted drilling fluid density	Actual drilling fluid density	Actual Bit Size used	Actual Casing Seating depth
	m	g/cm^3	g/cm^3	in (cm)	m
1	500	1.01	1.03	26 (66.04)	315
2	3703	1.37	1.04	17.5 (44.45)	2400
3	3917	1.82	2.15	12.25 (31.115)	3993
4	4644	1.88	1.88	8.5 (21.59)	4484
5	5224	1.71	1.62	5.9375 (15.08)	5224

6. Validation of Predicted and Real Field Data

In this section, the predicted and real Equivalent Mud Weight (EMW) and casing seating depths employing Eaton's Drilling results were compared, as can be seen in Table 1. Waha Company used about 1,379 kPa to 2,758 kPa (200 psi - 400 psi) as sustained pressure to ensure overbalance-drilling process. The gathered predicted results of 12 well were compared with the actual results of the deepest studied well in this research. Both the predicted and actual data show that five casing strings and drilling fluids are needed to drill a well in this area. It is evident that the predicted and real results are comparable, which confirms the accuracy of applying Eaton's drilling method to predict the formation pore and fracture pressure gradients, drilling fluid weight and casing seating depths.

7. Conclusion

The range of the formation pore pressure value is from less than hydrostatic pressure (normal pore pressure) to critically abnormal pressure (up to 90 % of the overburden pressure). The overall results provided that the drilling data are more reliable to be employed for predicting formation pressure gradients than the well-logging data. The predicted formation pressure gradients graph clearly shows the casing seating depths as well as the maximum and the minimum mud weight gradients that can be employed. So, the figure of the gathered data can be used as a reference for future drilling processes in the NC98 field-Sirte basin. Finally, all of the goals of this study were clearly addressed.

Nomenclature

Cr = rock matrix compressibility,

Cb = bulk compressibility of rock.

D = depth (m)

d_{bit} = bit diameter, (cm),

$d_{c,normal}$ = normalized dc-exponent value.

$d_{c,observed}$ = actual dc-exponent value.

Pp$_{normal}$ = normal formation pore pressure (kPa).

P$_F$ = formation fracture pressure (kPa).

ROP = Penetration Rate (m/h),

RPM = Round per minute,

WOB = Weight on the bit (lb),

σ_{ob} = overburden stress, kPa

ρ_{normal} = Normal Hydrostatic Gradient (g/cm^3),

ρ_{actual} = Current mud Weight (g/cm^3).

Δt_{normal} = normalized sonic transit time.

Δt = the actual obtained sonic transit time using sonic log tool.

σ_v = effective vertical stress, kPa

$\propto$ = Biot's constant, (0< $\propto$ <1) = (1- Cr/Cb)

$$v = \text{Poisson's ratio} = v = \frac{0.5 \times \left(\frac{\Delta ts}{\Delta tc}\right)^2 - 1}{\left(\frac{\Delta ts}{\Delta tc}\right)^2 - 1}$$

References

[1] Swarbrick, R.E., Osborne, M.J., Yardley, G.S.. Comparison of overpressure magnitude resulting from the main generating mechanisms. In: Huffman, A.R., Bowers, G.L. (Eds.), Pressure regimes in sedimentary basins and their prediction: AAPG Memoir. 2002, 76, 1–12.

[2] Bourgoyne (Jr), A.T., Millheim K.K., Chenevert M.E., Young (Jr), F.S. Applied drilling engineering. Richardson, Texas: revised 2nd printing. 1991, 246-250. (In United States of America)

[3] Jwngsar, B., Sircar, A, Karmakar, G. P. Pre-drill pore pressure prediction using seismic velocities data on flank and synclinal part of Atharamura anticline in the Eastern Tripura, India. J. Pet. Expl. Prod. Technol. https://doi.org/10.1007/s13202-013-0055-0.

[4] Helset, H. M., Lthje, M., Ojala, I., Lothe, A., Jordan, M., Berg, K., Nilssen, I. R. Improved pore pressure prediction from seismic data. In: Geopressure (EAGE), 2010, Presented at 72nd EAGE Conference and Exhibition incorporating SPE EUROPEC 10 June 2010, Barcelona, Spain.

[5] Akinbinu, V.A. Prediction of fracture gradient from formation pressures and depth using correlation and stepwise

multiple regression techniques. J. Pet. Sci. Eng. 2010, 72, 10-17. https://doi.org/10.1016/j.petrol.2010.02.003

[6] Dodson, J.K. Gulf of Mexico 'trouble time' creates major drilling expenses. Offshore. 2004, 64 (1).

[7] Zhang, J. Pore pressure prediction from well logs: methods, modifications, and new approaches. Earth-Science Reviews, 2011, 108, 50–63. https://doi.org/10.1016/j.earscirev.2011.06.001

[8] Green, S., Swarbrick, R., O'Connor, S., Clegg, P., Scott, D. T., Pindar, B. Pore pressure prediction in challenging areas-Reducing uncertainty by understanding rock behavior. In: AAPG Annual Convention, 2010, adapted from poster presentation at AAPG Annual Convention, New Orleans, Louisiana, 2010, 11-14 April.

[9] Dickinson, G. Geological aspects of abnormal reservoir pressures in Gulf Coast Louisiana. AAPG Bulletin.1953, 37, 410-432.

[10] Bowers, G. L. Determining an appropriate pore-pressure estimation strategy. In: Offshore Technology Conference, 2001, Offshore Technology Conference 30, April-3 May 2001, Houston, Texas, Paper OTC 13042. https://doi.org/10.4043/13042-MS

[11] Yardley, G.S., Swarbrick, R.E. Lateral transfer: a source of additional overpressure? Marine Pet. Geol.2000,17, 523-537. https://doi.org/10.1016/S0264-8172(00)00007-6

[12] Meng, Z., Zhang, J., Wang, R. In-situ stress, pore pressure and stress-dependent permeability in the Southern Qinshui Basin. Int. J. Rock Mech. Min. Sci. 2011, 48, 122-131. https://doi.org/10.1016/j.ijrmms.2010.10.003

[13] Saheel, A. S., Bin-Samsudin, A-R., Bin-Hamzah, U. Regional geological and tectonic structures of the Sirt basin from potential field data. Am J Sceint Indust Res. doi:10.5251/ajsir.2010.1.3.448.462

[14] Kendall, C., Alnaji, N., McCarney-Castle. Sirte Basin. (n.d.). Available at: http://www.sepmstrata.org/page.aspx?pageid=145. Accessed on: 15 February 2014. (In Canada)

[15] Waha Oil Company. The Geology Column of Gialo – NC98. Personal Communication. March 1st, 2007.

[16] Terzaghi, K., Peck R.B. Soil Mechanics In Engineering Practice. New York: J. Wiley, 1948. 87. (In United States of America)

[17] Baker Hughes INTEQ. Formation pressure evaluation-Reference Guide Houston: Baker Hughes INTEQ

Training and Development. 1996, 5-9. (In United States of America)

[18] Gardner, G.H.W., Gardner, L.W., Gregory, A.R. Formation velocity and density-A diagnostic basics for stratigraphic traps. Geophysics.1974, 39, 770-780.

[19] Yoshida, C., Ikeda, Eaton, B.A. An investigative study of recent technologies used for prediction, detection, and evaluation of abnormal formation pressure and fracture pressure in north and South America. In: Asia Pacific Drilling Technology, 1996, SPE/IADC Asia Pacific Drilling Technology, 9-11 September 1996, Kuala Lumpur, Malaysia. IADC/SPE 36381.

[20] Bowers, G.L. Pore pressure estimation from velocity data: accounting for overpressure mechanisms besides undercompaction. SPE Drill. Completions. 1995,10, 89-95.

[21] Jorden, J. R., Shirley, O. J. Application of drilling performance data to overpressure detection. J. Pet. Technol. 1966,18, 1387-1394. http://dx.doi.org/10.2118/1407-PA

[22] Bingham, M.G. A new approach to interpreting rock drillability. re-printed from Oil Gas J. 1965, 93.

[23] Rehm, B., Mcledon, R. Measurement of formation pressure from drilling data. In: Fall Meeting of the Society of Petroleum Engineers, 1971, Fall Meeting of the Society of Petroleum Engineers of AIME, 3-6 October 1971, New Orleans, Louisiana, SPE 3601.

[24] Eaton, B.A. The equation for geopressure prediction from well logs. In: Society of Petroleum Engineers, 1975, Fall Meeting Society of Petroleum Engineers of AIME, 28 September – 1 October 1975, Dallas, Texas, SPE 5544.

[25] Gruenwald, R. M., Buitrago, J., Dessay, J., Huffman, A., Moreno, C., Munoz, J. M. G., Diaz, C., Tawengi, K. S. Pore pressure prediction based on high resolution velocity Inversion in carbonate rocks, Offshore Sirte Basin, Libya. In: AAPG Annual Convention and Exhibition, 2010, Adapted from oral presentation at AAPG Annual Convention and Exhibition, April 11-14, New Orleans, Louisiana. DOI: 10.3997/2214-4609.201401145

[26] Kankanamge, T. Pore pressure and fracture pressure modelling with- OFFSET WELL DATA AND ITS APPLICATION TO-SURFACE casing design of a development well, deep Panuke gas pool offshore Nova Scotia. Master of Engineering. Dalhousie University Halifax, Nova Scotia, 2013. (In Canada)

REVIEW

Cost Estimation for Modernization of Metro Terminal Stations Using ANN Technique

Ahmed Abdelmoamen Khali[l]*   M. Abdel Rahman[2]

1. Faculty of Engineering, Shoubra Benha University, Shoubra, 11629, Egypt

2. Railway Track Engineer, Cairo Metro Company, Cairo, Egypt

ARTICLE INFO	ABSTRACT

The current situation of Cairo metro stations, especially terminal stations and its surrounding areas, has bad financial revenue and bad effect on environment. It is a major factor in increasing of noise, traffic jam and air pollution, in addition to, spreading of street vendors, collecting of random parking around these terminal stations. Thus, this paper proposed a methodology helping to apply multilateral investments in metro terminal stations for getting extra profits and decreasing the bad environmental effect of terminal stations and its surrounding areas. Hence, Helwan-Metro station on line 1 has been considered as a case study. Number of passengers at peak time, their ages, and their destinations, have been considered by making a field survey and a questionnaire. After collecting data and finalizing the surveying questionnaire, primary studies were done to modify and introduce a new proposal for Helwan-Metro station. The initial cost of the proposed project is predicted by using Artificial Neural Network technique using Just NN software. The investment feasibility achieved by consideration of Life Cycle Cost analysis and calculation of Net Present Value (NPV) of the proposed project.

1. Introduction

Metro stations attract large numbers of passengers daily who make different impacts on surrounding areas. These impacts usually appear around stations, sometimes around transit corridors and in some cases as a combination of both [1]. Therefore, during the recent decades, development of metro stations in urban regions has significantly affected spatial flows and urban mobility as well as spatial development of urban areas. Improving availability of employment nucleuses, retail districts and essential facilities for citizens is the most obvious impact of this development. Such positive impacts can raise land values around metro stations and consequently it can provide especial opportunities for urban textures to improve their quality [2, 3].

Nowadays, there is an increase in population and unemployment in Cairo, which leads to increase the private modes of transportation, for example, microbuses. These facilities move randomly in several places around metro stations and their surrounding streets that leading to traffic jams, also, closing many streets which founded from

---

Corresponding Author:

Ahmed Abdelmoamen Khalil

Faculty of Engineering, Shoubra Benha University, Shoubra, 11629, *Egypt*

Email: ahmed.khalil@feng.bu.edu.eg

several decades. Also unemployment led to presence of a lot of vendors inside metro cars and around metro stations. Because of their large numbers, almost areas around station have been closed as shown in Fig. 1. The result is bad environmental effect like noise pollution that reach to 85 dB at rush hours and air pollution emissions such CO, CO2, NO, NO_2, SO and SO_2 [4, 5]. This problem must be resolved with technical solution.

Figure 1. Current situation around Helwan terminal station

In practice, constrained capacity at many older stations creates a conflict between enhancing the retail offer and improving passenger flows, but station investment can address this in a number of ways [6]. At some stations, it may be possible to create additional space, for example by creating a separate concourse level, or reconfigure the layout so that there is a clear separation between retail and other areas. More generally, the provision of clear signing and consistent way finding within and beyond the station boundary, as well as the removal of clutter, can improve passenger flows and make passengers feel more relaxed [7].

It was focused on a number of possible applications of some solutions world-wide and on specific factors that allowed for their implementation. It concludes that commercial activity development at railway stations meets a certain number of criteria, the first obviously being that of size and volume for passenger traffic. The operators interviewed, as part of this study, agree on a minimum volume of traffic 50,000 passengers/day as a prerequisite for developing a "bankable" commercial activity. This does not, of course, mean that commercial activities cannot be developed in smaller stations, but the critical size mentioned above is the threshold based on which part of the financing can be raised in terms of commercial revenues [8].

In recent years, a number of major stations have been reconfigured with a view to increasing the retail and other services available. At London Paddington, the main retail offer is located off the main concourse, removed from the main passenger flow while remaining visible and ac-

cessible to both passengers and the non-travelling public. Similarly, at Manchester Piccadilly a number of retail outlets have been placed on a separate level, while others have been separated from the passenger circulation and waiting areas, and there are current plans for further improvement and expansion of the retail facilities at the upper concourse level. In some cases, the retail offer at the station has been transformed such that the station location is now a destination in its own right. The clearest example of this is St Pancras, where approximately one quarter of station users have no intention of catching a train and visit the station entirely for the shopping, cafes and restaurants. The same phenomenon can also be observed at major stations across continental Europe [9]. There is strong evidence that the perception and economic performance of an area can be enhanced by the presence of well-designed buildings, and there is no reason why stations should be an exception[9].

The concentration of passengers with time to spare at a station creates an attractive market for many retailers. This has been recognized for many years by a number of established retail organizations, notably W H Smith, which opened its first station based outlets during the railway boom of the 1840s. Today, station based retail businesses are significantly outperforming high street shops; recent Network Rail data indicate that retail sales at stations increased by 5% in the last quarter of 2010 as compared with a 0.4% increase on the high street [10]. The design of today's stations tends to be different in expression from their early age. Presently, they are often designed in such a manner as to take advantage of existing structures that affect the spatial planning [11]. Attention is greatly paid to problem-solving of their interior spaces. There are four main functional areas typically housed in most stations; core, transition, peripheral, and administrative areas [12].

More functions are integrated, and numbers of passengers are increased. The stations appear to be more than people-processors, but can expedite people's lifestyles. Similar to the design of airport terminals, the trend of the station design is to take full advantage of the time passengers wait around by providing facilities and entertainment. It is evident that many grand stations in the United States, Great Britain, and Japan begin to look like shopping districts that become tourist attractions. Many urban functions are brought inside the stations. It gives the opportunity to bring together restaurants, retail outlets, cafes, offices, currency exchanges, banks, post offices, car rental companies, movie theaters, and so on. The historic Union Station in Washington, D.C. is a good example of this concept. The 600,000 square foot space has been adaptively redesigned and renovated to become a major

retail, entertainment, and transportation center [2].

Helwan station is considered the case of study in this research as Helwan station and its surrounding area is one of the most stations that face this phenomenon because of spreading of slums, street vendors and random parking lots around the station. Thus, the bad effect on environment (noise, air pollution, visual pollution and traffic jam, etc.) has occurred. This research aims to use tools helping the authority of Cairo metro to make extra profit through investing in terminals, and to eliminate the phenomenon of street vendors inside and around metro stations. Thus, the authors propose a new project for transferring the old buildings to mega malls and car parking.

2. Material and Method

A field survey has been carried out by the authors, where, they counted the number of metro passengers, which arrive to Helwan-Metro station at peak times. Counting process has been done accurately in holidays and school time. Then, a sample of passengers has been selected to determine their ages and their genders. During holidays, the passengers have been asked about their destinations after exit from metro station to know number of parking lots that will be required and the number of required buses for each direction. Also, passengers have been asked about the number of days in which they use metro during week. After that, passengers have been asked about their opin-

ions in the street vendor's phenomenon around the station and their opinions in the random markets. The questionnaire that has been used in the interviews is attached in Appendix A.

The initial cost of the proposed project is predicted by using Artificial Neural Network technique using Just NN software through six steps namely: 1) Determining output variables ; 2) Identifying input variables; 3) Data collection and encoding ; 4) ANN Structure design ; 5) Training & validation, and 6) Cost calculation [13, 14]. The software, firstly, determines the specific output variable to be used in predicting a preliminary estimation of construction cost at the feasibility study stage. Hence, it identifies the critical input variables which affect the construction cost [15]. The input data represents the attributes of the problem available at the early stage of the projects, which may affect the final cost of construction. Data have been collected from 13 metro and railway station projects. These projects have some common characteristics, which enable the predicting of preliminary estimation for similar new project [16, 17]. The collected data were randomly divided into 2 sets; training data set and a validation data set [18, 19]. The historical data that has been entered to the software to make both training and validation process, is shown in Table 1, and data of the proposed project in Helwan station is given in Table 2.

Table 1. Historical data within Just NN environment

No.	Project name	Area	No. of Floor	Park	Start Date	Const. duration	Marble Face	Mall	Output
P1	Cambridge station	17678	2	450	2016	2	True	False	52000000
P2	Williams landing	3700	3	500	2013	2	False	False	86000000
P3	Cairo station	17000	3	300	2013	3	False	False	34285000
P4	Sedy Gaber station	16250	3	850	2013	3	True	True	32143000
P5	Hadayek el Maady	3200	2	0	2014	4	True	True	6580000
P6	Mansheyt el Sadr	1800	2	0	2012	2	True	True	38500000
P7	New Delhi station	9000	3	800	2009	2	False	True	972000000
P8	Berlin station	70000	5	870	2006	11	False	True	1000000000
P9	Laverton station	11000	1	400	2011	3	True	False	96200000
P10	Hamburg St. station	27800	2	0	1991	6	False	True	6000000
P11	Northampton station	30500	3	1270	2015	1	False	True	40000000
P12	Franklin St. station	36910	2	750	2007	3	True	False	35000000
P13	Napoli train station	20000	5	1300	2012	9	False	True	70000000

Table 2. Data of the proposed project

No.	Project name	Area	No. of Floor	Park	Start Date	Const. duration	Marble Facade	Mall	Output
Q:13		3400	6	850	2016	2	True	True	Required

3. Analysis

3.1 Analyzing the Field Survey Data

Analyzing the collected data and regarding the recorded answers in the questionnaire, it is found that passengers with ages between 24 and 60 years use metro mostly in holiday time and school time. The percentage of students with ages between 18 and 24 years doesn't exceed 7%.Whereas, during the school time this percentage reaches 15% of the total number of passengers. It is, also, found that most of passenger's destinations, after arriving Helwan station, are to other suburbs (Tebin – El Saff – Arab Ghonim – Ezbet el Walda – 15 may city – American project), in addition to original Helwan habitants. It is, also, found that distribution of passengers on those destinations are 15 may 29%, El Saff region 17%, El Tebin region 15%, American Project region 5% from the total number of passengers as shown in Fig. 2. The percentage of Helwan habitants is about 11%. The percentage of passengers distributed along the week days is shown in Fig. 3.
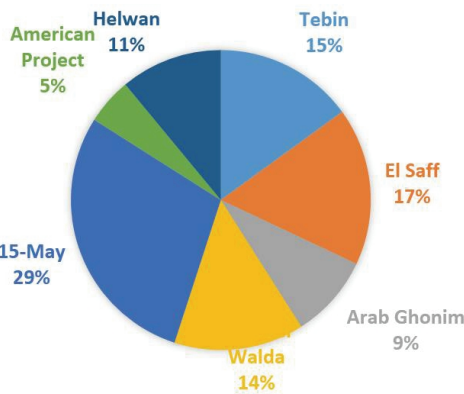

Figure 2. Passenger's destinations after passing Helwan station, from 14 pm to 17 pm
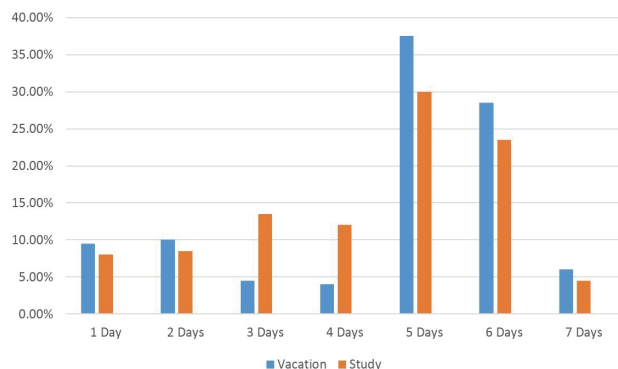

Figure 3. Numbers of passengers riding Metro from Helwan station during week

The interviewed passengers have been also asked about their opinions in the street vendor's phenomenon around station to determine their reaction with them. The answer

was 25% almost of total number of passengers is impossible to buy from the street vendors even they are in a necessary need to buy. In contrary, the ratio of passengers who always buy from these random vendors which located around metro station was about 20%. Ratios of different answers of the passengers during school session and school vacancies are shown in Figs 4 and 5 respectively.

The remaining ratio of passengers (about 55%) sometimes has to buy from these street vendors when coming-out of the station as they are tired or in hurry, except for that they prefer buying from specialized places for the commodities they want. Most of the passengers recorded that street vendors' phenomenon around metro stations is indication of uncivilized phenomenon, as it, also, helps in increasing chaos and spread of bullying around the station, and it makes people feel unsafe. Introducing the idea of the proposed project to the asked passengers, it was found that most of them are deeply interested in the idea, and hope to finish this project as soon as possible. The proposed project will save their time and increase their safety in the streets, as well as, it will save their needs (stationery, food, clothes, transport means) in one building.
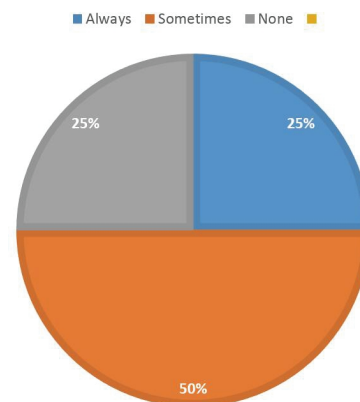

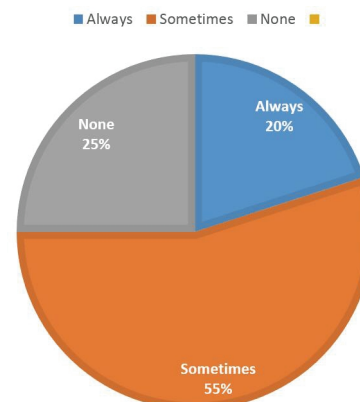**Figure 4.** Shopping from Helwan Square during school session

Figure 5. Shopping from Helwan Square during school vacancies

3.2 Cost Estimation

After assigning the minimum accepted error (4%), ANN software starts to make the learning cycles of a training data set of 11 projects which from project 1 to 13 except projects 5&12 and a validation data set of 2 projects which are 5&12 to check the error. ANN chooses one hidden layer with five nodes to get the optimum result. Fig. 6 shows the weights for the network's inputs and Fig. 7 shows the graphical presentation of the network layers.

Fig. 8 illustrates the minimum, maximum and average error for learning within the learning cycles. In addition, this Figure shows the validating error for the system. Where: The horizontal axis is nonlinear to allow the whole learning progress to be displayed. As more cycles are executed the graph is squashed to the right. The red line is the maximum example error, the blue line is the minimum example error and the green line is the average example error. The orange line is the average validating error. When the Total Net Error value drops below the max error, the training is complete.
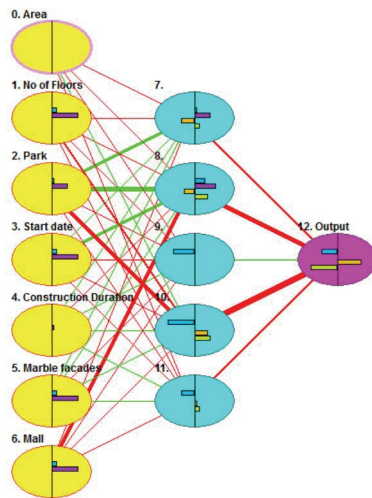

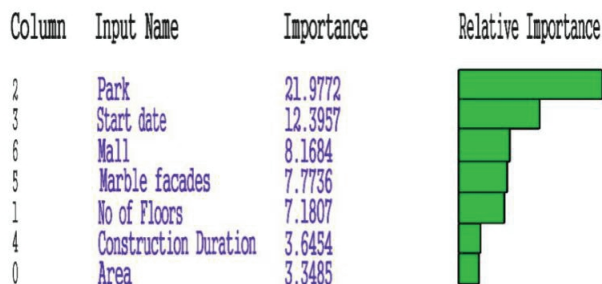**Figure 6.** Relations between parameters
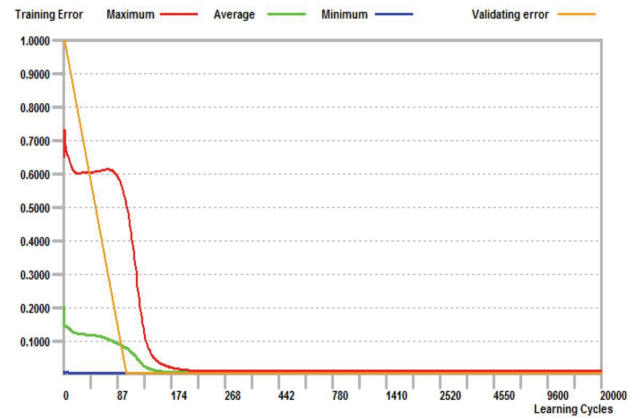

Figure 7. Importance of parameters

Figure 8. Error of the process

After running the program and getting the acceptable value of error, it is possible to calculate the construction cost of any new project. As a result, the initial construction cost of the proposed project is approximately $12,800,000 96,000,000L.E.

3.3 Net Present Value of the Proposed Project

Net Present Value has been calculated for the new building in Helwan-Metro station to get the total revenue of the project. Time value of money can be used to bring all future cash flows to their present-day equivalent value by Net Present Value. Therefore, the Length of study period is taken to be the operational lifetime of the station (i.e. 50 years) the interest rate (i) =18 %.

Equation 1 has been used to calculate the Net Present Value of the project:

$$\text{NPV} = -\,\text{PV (I)} - \text{PV (A)} - \text{PV (N)} + \text{PV (M)} + \text{PV (T)} \quad (1)$$

Where:

PV (I) is present value of initial costs;

PV (A) is present value of annual operation, maintenance, utility and other costs;

PV (N) is non-annual, operation, maintenance, utility and other costs.

PV (M) is present value of mall and parking cars, and

PV (T) is present value of tickets.

3.3.1 Annual Costs

The annual costs represent the costs required annually to cover operation, maintenance, utility works for the station. Equation 2 is used to calculate these costs. According to the Egyptian company of Cairo metro, the annual costs are 800,000 L.E. with annual up gradient 5 %.

$$\text{PV (A)} = A \left[\frac{1 - (\frac{1 + g1}{1 + i})^{n}}{i - g1} \right] \quad (2)$$

Therefore, present value of operation maintenance cost is calculated using equation 2:

$$PV(A) = 800,000 \left[\frac{1 - (\frac{1 + 0.05}{1 + 0.18})^{50}}{0.18 - 0.05} \right] = 6,135,877.679 \text{ L.E}$$

3.3.2 Non Annual Costs

Non Annual Costs refer to the periodic costs required to cover the operation, maintenance, utility for the station every five years. Equation 3 is used to calculate these costs. The Egyptian company of Cairo metro needs to approximately L.E. 3,000,000 every 5 years to cover these works. Using the interest tables, the present value of non-annual operation and maintenance cost is:

$$PV(N) = F \left[{}^{A}/_{F}, i, n \right] \left[{}^{P}/_{A}, i, n \right] \tag{3}$$

$$PV(N) = 3,000,000 \left[{}^{A}/_{F}, 18, 5 \right] \left[{}^{P}/_{A}, 18, 50 \right]$$

$$PV(N) = 3,000,000 [0.13978][5.5541] = 2,329,056.29 \text{ L.E}$$

3.3.3 Estimation of Annual Revenues

To calculate the total present value of benefits from the mall and parking in the proposed project, it is considered that annual rent value is 12,000,000 L.E. Where, the total area is 12,000 m2 and the revenue of one square meter is assumed to be 100 L.E. as per the predominant prices. Substituting in Equation 4, the present value of renting is obtained.

$$PV(M) = M \left[\frac{(1 + i)^{\wedge}n - 1}{i(1 + i)^{\wedge}n} \right] \tag{4}$$

For that, the present value of mall and parking cars (M) =

$$PV(M) = 12,000,000 \left[\frac{(1 + 0.18)^{\wedge}50 - 1}{0.18(1 + 0.18)^{\wedge}50} \right] = 66,649,692 \text{ L.E}$$

The annual benefits of tickets sales in Helwan station is calculated based on the number of passengers that are approximately 36,050,000 person and unit price of the ticket. Thus, the annual revenue of tickets equals 36,050,000 L.E. with annual up gradient 3.5 % due to increase in number of passengers. Equation 5 is used to calculate these benefits.

The present value of ticket sales is:

$$PV(T) = T \left[\frac{1 - (\frac{1 + g3}{1 + i})^{n}}{i - g3} \right] \tag{5}$$

$$PV(T) = 36,050,000 \left[\frac{1 - (\frac{1 + 0.035}{1 + 0.18})^{50}}{0.18 - 0.035} \right] = 248,267,136.8 \text{ L.E}$$

Substituting in equation number 1 with the obtained values of costs and revenues, the net present value of the proposed project is calculated as follows,

NPV = 210,451,894.8 L.E.

The conclusions of this research can be summarized as follows:

1) Multilateral investment in metro stations has positive impact especially, in terminal stations.

2) Factors affecting the overcrowdings and traffic jam around old terminal stations, as the case of Helwan Station, include:

Old planning and design of the station buildings and services.

Lack of civilized areas which dedicated as parking lots.

Spread of street vendors in random places around the station.

Lack of available accesses to the station.

3) It's found that 89 % of passengers are not residents in Helwan city, but they are living in districts which are 2 to 15 km from Helwan station. Those passengers need transport means from Helwan station to their destinations. Thus, they contribute in a very heavy crowdedness, traffic jam, environmental pollution and bad sight-seeing around the station.

4) I's found that 11 % of the passengers living in Helwan city i.e. close to the station by a distance not more than 1 km. Hence, they don't need transportation mean to go to their destinations and they don't need to make shopping from the random street vendors.

5) To reduce the pollutions in Helwan station zone, it's found necessary to consider the following procedures:

Separation of metro passengers from surrounding station streets through exploitation of available spaces into constructing a building, which contains parking areas and commercial mall. Thereby, it will prevent the spread of street vendors around the station and taking them to shops in mall.

Transfer the positions of random cars in the streets surrounding the station to the dedicated areas in the proposed building.

6) The initial cost of the proposed project in Helwan station has been estimated by Artificial Neural Network program using just-NN software compared with local and global projects.

7) Calculating the Net Present Value for total costs of investment and the total revenue from the proposed solution, it is found that:

Construction cost of the project = 96,000,000 L.E.

Net Present Value of the project = 210,451,894.8 L.E.

Total annual revenue of the project = 12,000,000 L.E.

Annual revenue of 1 meter square = 1,200 L.E.

Monthly cost of parking 1 car = 700 L.E.

Rent value of 1 shop per month = 600 L.E.

works. Also, we are very thankful for colleagues who have assisted in carrying out the survey works.

References

[1] Neville, M. and Albert, H. "What Makes A Good Secondary Shopping Center? A Shopping Centre Management", 2013.

[2] Cervero, R., Murphy, S., Ferrell, C., Goguts, N., Tsai, Y., Arrington, G. et al., "Transit-oriented development in the United States: Experiences, challenges, and prospects", (TCRP 102). Washington, DC: Transportation Research Board, 2004.

[3] Lin Z., Theingi S., and Maung, H., "Studies of the Status of Central Business District Area (CBD) in Yangon, Myanmar", International Journal of Emerging Technology and Advanced Engineering, 2014, 4(5).

[4] Ahmed Khalil."Engineering of Railways and Metro lines", 1st. edition, Scientific Book House, 2009.

[5] Arrington, G. B. and Cervero, R., "Effects of TOD on Housing, Parking and Travel", Transportation Research Board, 2008, 1-58.

[6] Paul P.,"Investment in stations, a guide for promoters and developers", (Version 2.0). Network Rail, 2011.

[7] S. D. Gleave. "The value of Station Investment, Research on regenerative impacts", A report submitted to Network Rail. 2011.

[8] PWC. "Which financial mechanisms for urban railway stations?", A study has been submitted to La Fabrique de la Cite, 2013.

[9] Cabe and Detr., "The value of Urban Design", 2001.

[10] Network Rail., Annual Report,2011.

[11] S. Fuller. "Life-Cycle Cost Analysis (LCCA), Whole Building Design Guide (WBDG)", National Institute of Building Science, 2010, [Online]. Available: http://www.wbdg.org/resources/lcca.php.

[12] S. Kandee."Intermodal Concept in Railway Station Design", www.bu.ac.th/knowledgecenter/epaper/jan_june2004/somruedee.pdf, (Accessed August 2015)

[13] Saumya B., Kreeti J., and Neeti J., "Artificial Neural Networks", International Journal of Soft Computing and Engineering (IJSCE), ISSN: 2231-2307, 2011, 1, Issue-NCAI2011, India.

[14] Dimiter D., "A Definition of Artificial Intelligence", Institute of Mathematics and Informatics, Bulgarian Academy of Sciences, Sofia 1090, Bulgaria, 2004.

[15] Megha J., and K.K., Pathak. "Applications of Artificial Neural Network in Construction Engineering and Management-A Review", International Journal of Engineering Technology, Management and Applied Sciences, 2014, 2(3), ISSN 2349-4476.

[16] Mohammad H. Bataineh. "Artificial neural network for studying human performance", University of Iowa, 2012.

[17] Mequanint B. and Tesfu A., "Railway Mini-Station Design at Minlik Square", School of Electrical and Computer Engineering Railway System Planning and Operations Management [MEng 6409], 2005.

[18] Michael N, "Neural Networks and Deep Learning", 1st edition, 2014, 2-37.

[19] Ismaail S., Hossam H., and Mohammed A. R., "A Neural Network Model for Construction Projects Site Overhead Cost Estimating in Egypt", IJCSI International Journal of Computer Science Issues,2011, 8(3), 1, ISSN (Online): 1694-0814.

Appendix A. The questionnaire (translated from Arabic)

No	Question	Option		Option		Option		Option	
1	Do you usually travel with the metro?	Yes	☐	No	☐	Sometimes	☐		
2	How many times do you travel with metro within a week?	1	☐						
		2	☐						
		3	☐						
		4	☐						
		5	☐						
		6	☐						
		7	☐						
3	Which is more, your travelling with metro during school time or in holidays?	Holidays	☐	School time	☐	Equal	☐		
4	Do you only take Line No. 1 or change with other metro lines in one trip?	Line 1	☐	Change	☐				
5	Do you use other transport means than the metro lines in your trips?	Yes	☐	No	☐	Sometimes	☐		
6	What is your working job?	employee	☐	Student	☐	Other	☐		
7	Gender	Male	☐	Female	☐				
8	How old are you?								
9	Where do you live?	Helwan	☐						
		15 May	☐						
		Tebin	☐						
		El Saff	☐						
		El Walda	☐						
		Arab Ghonim	☐						
		American Project	☐						
		Other	☐						
10	Is your work far from Helwan?	Yes	☐	No	☐				
11	Do you come back to your home daily?	Yes	☐	No	☐	Every week	☐	Other	☐
12	Do you buy from the random venders around metro station?	Yes	☐	No	☐	Sometimes	☐		
13	What kind of your purchases from around metro station?								

REVIEW

Effect of Aromatic Ring, Cation, and Anion Types of Ionic Liquids on Heavy Oil Recovery

Ahmed Tunnish[1]*   Amr Henni[2]   Ezeddin Shirif[1]

1. Petroleum Systems Engineering Department, Faculty of Engineering, University of Regina, Canada.

2. Process Systems Engineering, Faculty of Engineering and Applied Science, University of Regina

ARTICLE INFO	ABSTRACT

Surfactant/alkali flooding is one of the best chemical flooding methods to enhance the oil Recovery Factor (RF). In this research, Ionic Liquid/Alkali (ILA) mixtures were chosen to represent a form of chemical flooding experiments. The selected Ionic Liquids (ILs), {[EMIM][Cl], [THTDPH][Cl], [EMIM][Ac], [BzMIM][Cl], [DMIM][Cl], [BzMIM][TOS], [dMIM][TOS] and [MPyr][TOS]}, were introduced to investigate their efficiency in improving heavy oil (14o API) RF from the sand packs. Besides, the use of mixtures of the same ionic liquids and brine (3.37 wt. % salts) with an alkali (Sodium Bicarbonate [$NaHCO_3$]) were also investigated. In this experimental study, the flooding process started with injecting about 3.2 Pore Volumes (PVs) of only brine, followed by one PV of the chemical composites, and flushed with two PVs of formation brine. The study discussed the influence of cation type, anion type, the structure of the ILs, and the effect of combining ILs/alkali on the RF. The results revealed that the proposed chemical mixtures are effective in enhancing the recovery factor. ILs with shorter alkyl chain and more aromatic rings are noticeably more efficient in enhancing the RF. Finding the optimum composition of ([DMIM][Cl] + $NaHCO_3$) the chemical slug increased the additional RF up to 31.55 (% OOIP). Also, increasing the slug size to two PVs improved the RF to 42.13 (% OOIP). The recovery factor mechanism was explained and supported by measuring the effect of IL types on the viscosity, Surface Tension (SFT), and Zeta Potential (ZP) of the mixture.

1. Introduction

Due to the challenges and high cost that are needed to explore and develop new reservoirs, oil corporations began investigating new ways where the produced oil ratio of the depleted or non-producing reservoirs would be developed.[1] It is well known that roughly, conventional reservoir forces would produce one-third of the Oil Initially In Place (OIIP). That is why Enhanced Oil Recovery (EOR) methods are required to produce more of the remaining oil.[2] One of the suggested methods is to flood the reservoirs with chemicals such as surfactants. Due to the positive results of the chemical EOR techniques, they have been commonly employed for the last three decades.[3] Surfactants can reduce the interfacial ten-

*Corresponding Author:
Ahmed Tunnish
Petroleum Systems Engineering, Faculty of Engineering and Applied Science, University of Regina, Regina, Canada.
E-mail: tunnisha@uregina.ca

sion (IFT) of oil-water systems to ultralow levels, which, in turn, increases the RF.[4,5]

Surfactants are composites that have hydrophilic (head) and hydrophobic (tail) groups. [6] They are capable of lowering the IFT and alter the rock wettability.[7] Recently, a new class of chemicals considered as surfactants were introduced namely Ionic Liquids (ILs). They are made of cation (organic) and anion (organic or inorganic).[8, 9] The types of cations and anions control their properties.[10] Besides, ILs have low vapor pressures and are chemically and thermally stable even when injected in reservoirs with high pressures and temperatures.[11] ILs possess a significant density, polarity, and heat potential.[12,13] Most of ILs withstand water and have low toxicity.[14] ILs also can lower the oil-water IFT. It was observed that the IFT reduction increased with developing IL concentration. Even with the presence of salts (NaCl, Mg_2Fl), IL still noticeably decreases the IFT.[15] The addition of salt (NaCl) to the mixture of the low ratio of surfactant might reduce the surfactant head group area and affect the surfactant interfacial adsorption performance. In opposition, when salt was added to high surfactant ratio, it increased the micelle solubilization. Besides, IL with longer alkyl chain on the cation size has better performance in reducing the IFT. [16] ILs can alter the wettability to more water wet, which is preferred for improving the RF.[17,18] The adsorption of surfactant increased as the ratio of surfactant developed to the critical micelle concentration, but exceeding that concentration, no more improvement in the adsorption noticed. The electrostatic interaction between the surfactant's headgroup charge and net charge on the surface of the rock might be the main reason of adsorbing the surfactant and altering the wettability. So IL could adsorb on the rock surface and release the crude oil.[17]

This work reports chemical enhanced heavy oil recovery (CEHOR) employing ionic liquid/alkali (IL/A). Different chemically structured ILs were mixed, for the first time, with alkali ($NaHCO_3$) and employed for EHOR. Many properties such as viscosity, SFT and ZP denoted studied and correlated to changes in RF. The upside of IL injection is the fact that it does not demand high pressure or temperature to produce the heavy oil.

2. Materials

Chemical types applied in the study were alkali (Sodium Bicarbonate [$NaHCO_3$]), 1-Ethyl-3-MethylIMidazolium Chloride [EMIM][Cl] (≥ 98 % mass), 1-Benzyl-3-MethylIMidazolium Chloride [BzMIM][Cl] (≥ 97 % mass), and TriHexylTetraDecyl Phosphonium Chloride [THTDPh][Cl] (≥ 95 % mass) were obtained from Sigma-Aldrich Company; 1-Ethyl-3-MethylIMidazolium Acetate [EMIM][Ac] (≥ 95 % mass), and 1-Dodecyl-3-methylim-

idazolium Chloride [DMIM][Cl] (> 98 % mass) were purchased from IoLiTech Company, and 1,3-dimethylimidazolium Tosylate [dMIM][TOS] (≥ 98 % mass), 1-Benzyl-3-MethylIMidazolium Tosylate [BzMIM][TOS] (≥ 99 % mass), The Tosylate [Mpyr][TOS] (> 98 % mass) were acquired from Shanghai Cheng Jie Chemical Company LTD and used without any further purification. The chemical structures of the ionic liquids are presented in Fig. 1. Also, the composition of Synthesized Pelican Brine (SPB) injected is as shown in Table 1. Pelican Lake pool is the source of the used heavy oil sample. Table 2 presents the properties of the oil sample as reported by the Saskatchewan Research Council (SRC). Centrifuging the oil sample at high speed treated the fine solid particles. Finally, the sand pack samples were prepared using Ottawa sand with mesh size ranges from 40 to 80.

Table 1. The composition of Pelican brine (SPB)

Chloride, mg/l	20,607
Sulfate, mg/l	2
Sodium, mg/l	12,349
Calcium, mg/l	380
Magnesium, mg/l	280
Potassium, mg/l	80
TDS	33,698

Table 2. Pelican oil properties

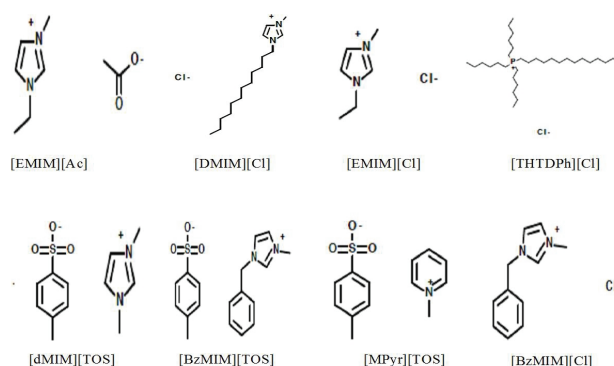| Density, g/cm³	@25°C	0.9642
Viscosity, cP	@22°C	1200
SARA, wt. %	Saturates	26.3
	Aromatics	39.7
	Resins	14.4
	Asphaltenes	11.4

Figure 1. The chemical structure of ionic liquids and commercial surfactant

3. Preparation and Methodology

3.1 Mixture Preparation and Properties Measurements

The samples were prepared at room temperature (21.5 ± 1 oC), and their characteristics were measured. First, type 1 ultrapure water instrument was used to prepare Distilled Water (DW) that were used to formulate the brine (SPB) and the chemical mixtures by mixing them using a stirrer for 20-25 minutes. Solution was checked for stability of the emulsion before the ZP, SFT, and viscosity were measured using Nano Zetasizer-ZS, KRUSS K100, and Brookfield DV-II viscometer, respectively.

3.2 Sandpack Samples Preparation

The traditional core flooding apparatus that consists of a pump, transfer cylinders, pressure gauge, core holder, and tubes was employed for the runs. The holder length and diameter are 7.4 cm and 3.3 cm, respectively. The sample was cleaned, dried, and the sand was dry packed, and the holder was vibrated. Fresh Ottawa sand was used for each experiment to have comparable wettability for all core samples. After vacuuming and saturating the sample with brine, the porosity and permeability were calculated. Pelican oil was then added continuously from the top into the sand pack at a rate of 1 cm3/min till the displaced water ceased to exit the core. The replaced and residual brine describes the initial oil saturation (Soi), and irreducible water saturation (Swirr), respectively. The petrophysical properties of the sand packs are presented in Table 3.

Table 3. Sand pack samples properties

Ka, D	5.36 ± 0.33
PV, cm^3	25.72 ± 0.33
Ø, %	40.61 ± 0.21
Swi, %	10.10 ± 0.38
Vo, cm^3	23.11 ± 0.14
Soi, %	89.90 ± 0.39

3.3 Flooding Procedure

The flooding mode started with injecting about 3.2 PV of brine (SPB), followed by 1 PV of a chemical slug (ionic liquid/alkali) and flushed with 2 PV of SPB. The flooding rate applied for all experiments was 0.75 cm3/min. The produced oil samples were gathered in testing tubes and put in a separator. The produced oil volume out of the original volume in the core sample is considered as the RF.

4. Results and Discussion

4.1 Effect of the Type of Anion/Cation/Alkyl Chain on the Performance of ILs

Several types of ILs were considered regarding enhancing the RF. As shown in Fig. 2, the RFs of flooding the sand packs with 3.2 ± 0.1 PVs of brine (SPB) were comparable (39.29 ± 0.24 % OOIP). Then the RF obtained by injection of 1 PV of chemical slug (1,000 ppm IL + SPB) mixture and 2 PVs of SPB that were used to flush the sample depending on IL type. The performance of the investigated ILs on improving the RF decreases in this order: [EMIM][Cl] (14.75 % OOIP) > [EMIM][Ac] (12.55 % OOIP) > [dMIM][TOS] (11.76 % OOIP) > [DMIM][Cl] (10.89 % OOIP) > [BzMIM][TOS] (10.22 % OOIP) > [MPyr][TOS] (10.00 % OOIP) > [BzMIM][Cl] (8.44 % OOIP) > [THT-DPh][Cl] (7.87 % OOIP). Nevertheless, it is clear that the additional RF improvement mainly depends on the IL type. The possible mechanisms for the enhancement could be due to lower SFT, ZP close to zero line, and increased viscosity of the introduced phases comparing to that of just SPB, as shown in Fig. 3 and supplementary material (S1). It is obvious that the addition of IL notably lowered mixture the SFT (73.062 mN/m) and increased both the ZP (-13.10 mV) and slightly the viscosity (1.08 cP) of the aqueous phase. Any of those factors could be the primary mechanism for the enhancement in the recovery factor when IL was combined with brine. Although the SFT represents the interfacial tension between air and liquid, it gives an idea about the efficiency of surfactants in reducing the IFT of two liquids. Tunnish found that [DMIM][Cl] is more active than [EMIM][Ac] in diminishing Pelican oil-brine IFT, and similar performance of these ILs was noticed in SFT measurements.[19] In this work, it is noticed that all ILs were capable of reducing the SFT. ZP represents the surface charge mechanism, and it completely agrees with the enhancement in the RF, as it is greater for the best RFs. Tunnish et al. noted that the RF enhanced as the ZP of the displacing phase increased.[20] As known, the zeta potential measures the repulsive or attractive forces between particles that address the stability of disperse systems. Fazullin and his colleagues observed that the gathering of oil products grew as the zeta potential decreased[21] in the case of cleaning up the produced water. Increasing the zeta potential of the injected mixtures might weaken the aggregation of the oil contents in the produced phase and form an emulsion. As highlighted in this study, the higher the ZP, the better it is for the RF, which represents weak aggregation, and the consequent creation of emulsion and carrying more oil out of the porous medium. The electrostatic interactions mechanism (wettability change)

represented by the ZP could be one of the factors that improved the RF in this study. Recently, Tunnish et al. found that the ZP value of different systems (brine/oil/sand) was mainly affected by the presence of IL. Adding IL to brine-oil and brine-oil-sand systems increased their ZP values. ILs "neutralize" the charge of the tested system, and may, consequently, alter the wettability type.[22] In a recent study, the addition of the type of an ionic liquid (Deep Eutectic Solvent) altered the rock wettability type and increased the RF, and was considered as a primary mechanism for EOR. Another suggested mechanism that led to an enhancement in RF is the increase in viscous force.[23] This led to a lower oil-water mobility ratio due to the addition of ILs.[24] In our case, as displayed in Fig. 3, all combined ILs led to an increase in the viscosity of the displacing phases. Although the difference is not too high to critically change the mobility ratio, it could be partially engaging in the noticed enhancement of the RF. Certainly, the ability of ILs to efficiently change the mobility ratio is stronger with oils with higher API values.
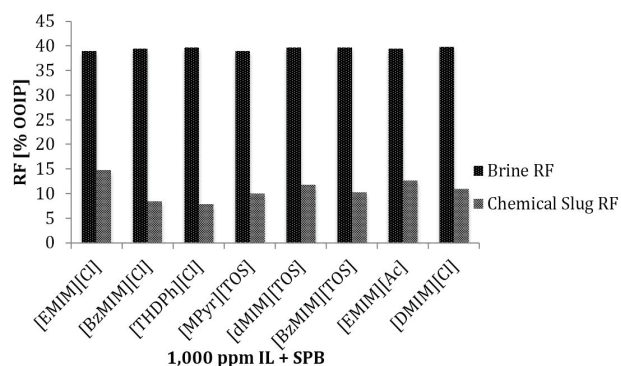

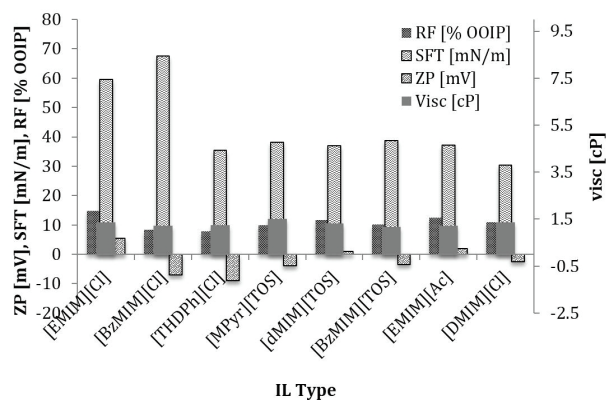**Figure 2.** The effect of IL type on the additional RF

Figure 3. The effect of ionic liquid type on the properties of ionic liquids

[Cl], [TOS] and [Ac] types of anions based ILs were selected to study the effect of the anion type on the RF.

Fig. 2 shows that the efficiency of 1 PV (1,000 ppm) of the selected ILs decreases as following: [EMIM][Cl] (14.75 % OOIP) > [EMIM][Ac] (12.55 % OOIP) > [BzMIM] [TOS] (10.22 % OOIP) > [BzMIM][Cl] (8.44 % OOIP). Regarding those results, we can say that when the same cation combined with an aromatic anion ([BzMIM][TOS]) is stronger than the non-aromatic ringed anion-based IL ([BzMIM][Cl]) in improving the RF. It could be because of the interaction between the aromatic compounds in the oil sample and ILs, which supports the effect of the aromaticity (π-π interaction) mechanism.[25] In comparison to one-sided aromatic IL ([BzMIM][Cl]), the tosylate anion as aromatic anion and the two aromatic rings on the cation may have stronger potential to interact with oil sample aromatics and progresses the RF noticeably. It was noticed that [EMIM] cation-based IL is more efficient when it is combined with [Cl] anion compared to that when it is united with [Ac] anion. It could be due to the high salinity ratio of the employed brine, as the efficiency of [EMIM] [Ac] improves with decreases the salinity ratio.[19]

Three cation types based ILs were chosen to study the influence of cation type on the performance of ILs. As shown in Fig. 2, the enhancement of RF by injecting 1 PV (1,000 ppm) of these ILs declines in the following order: [BzMIM][TOS] (10.22 % OOIP) > [MPyr][TOS] (10.00 % OOIP) > [BzMIM][Cl] (8.44 % OOIP) > [THTDPh][Cl] (7.87 % OOIP). Concerning ILs with the same anion base, the aromatic IL type (imidazolium) is more efficient than the aliphatic (phosphonium) cation IL, and that supports the potential of the aromaticity (π-π) mechanism. Regarding the number of aromatic rings, the IL with three aromatic rings ([BzMIM][TOS]) is more efficient than that of two aromatic ringed IL ([MPyr][TOS]).

The effect of cation alkyl chain type on the additional RF was also studied. Fig. 2 displays the efficiency of the ILs (1 PV and 1,000 ppm) decreases in the following order: [EMIM][Cl] (14.75 % OOIP) > [EMIM][Ac] (12.55 % OOIP) > [DMIM][TOS] (11.76 % OOIP) > [BzMIM] [TOS] (10.22 % OOIP) > [DMIM][Cl] (10.89 % OOIP) > [BzMIM][Cl] (8.44 % OOIP). For similar anion-based ILs, the shorter alkyl chain, the better is the RF. For the studied ILs and regardless of the anion type, it was observed that the ethyl type of alkyl chain was more efficient than all others.

This study confirms the great ability of ILs in improving the RF of heavy oil and the influence of ILs structure and composition (anion, cation and alkyl chain types) on their performances. The effect of four mechanisms (IFT/SFT, electrostatic, aromaticity, and viscous force) on the RF was discussed. The reduction in the SFT values somehow confirms the ability of ILs in reducing IFT. The slight

increase of the mixtures viscosity values confirms that the enhancement of RF, in this case, is not due to the contribution, as the primary mechanism, of the viscous forces. The improvement in the additional RF was stronger when highly aromatic, and higher ZP ILs were injected, which supports the contribution of the aromaticity interactions and electrostatic (wettability alteration) mechanisms in enhancing the RF.

4.2 Effect of NaHCO3 on the Performance of ILs

ILs were finally mixed with alkali (NaHCO$_3$) and introduced for enhancing the RF. Fig. 4 shows the RF (39.25 ± 0.26 % OOIP) of the first stage of the flooding process that began with injecting about 3.2 PVs of brine (SPB). Then, the additional RF after introducing 1 PV of chemical slug (1,000 (ppm) IL + 0.1 wt. % NaHCO3 + SPB) and flushing the sand packs with 2 PVs of SPB. The additional RF of the second step declined in the following order: [DMIM][Cl] (31.57 % OOIP) > [EMIM][Cl] (19.48 % OOIP) > [BzMIM][Cl] (18.42 % OOIP) > [THTDPh][Cl] (15.79 % OOIP) > [BzMIM][TOS] (14.13 % OOIP) > [EMIM][Ac] (13.44 % OOIP) > [dMIM][TOS] (13.25 % OOIP) > [MPyr][TOS] (12.61 % OOIP). In comparison to the injection of alkali alone (7.67 % OOIP), it is obvious that the additional RF is enhanced for all cases when IL was introduced. Similar results of adding just ILs to brine were noticed when ILs and alkali were added to the brine, where all mixtures improved the ZP and viscosity and reduced their SFT values, as shown in Fig. 5 and in the table provided in the supplementary material (S2). The anion and cation types control the performance of IL. Based on the additional RF results, RF is better when chloride [Cl] based ILs are injected. Concerning the cation type, it was found that imidazolium-based cation + [Cl] anion is considerably better than IL-based phosphonium cation + [Cl]. Remarkably, [DMIM][Cl] + NaHCO3 + SPB (31.55 % OOIP) mixture is more effective than all other combinations; one of the factors could be the higher ability of [DMIM][Cl] to increase the mixture viscosity (1.70 cP) further than the other mixtures. Also, the strength of cationic IL ([DMIM][Cl]) to decrease the SFT (28.99 mN/m) and increase ZP (15.21 mV) much more than the other selected ILs, as reported in Fig 5. Also, the potential of cationic IL as [DMIM][Cl] to create an emulsion is surely one of the reasons that led to the noticeable RF.[26] In another study, it was observed that the hydrophilic anion ([Cl]) based imidazolium IL was not efficient demulsifier,[27] which good for EOR purposes. Cationic surfactants have a positive head group and get strongly adsorbed in sandstone rocks[28] and change the wettability, which is another factor of improving the RF in the case of

[DMIM][Cl] (cationic IL). It is known that the addition of alkali to chemical slug helps to keep the ratio of surfactant in the mixture at the same level, which would raise the RF further.[29] An in situ surfactant is formed when an alkali reacts with the acid groups in the oil sample.[30,31] The ratio of surfactant adsorption and IFT decreased when alkali and surfactant were combined.[32,33]

This study proved the efficiency of injecting ILs either alone or combined with other chemical types (alkali) to improve the heavy oil recovery. It is evident that more than one mechanism (IFT/SFT, electrostatic, aromaticity, and viscous force) is controlling the noticeable enhancement in the RF. For ILs with similar cations or anions types, the one with more aromatic rings is better for RF improvement. The optimum slug composition was obtained in this research, where 1 PV of ([DMIM][Cl] + NaHCO$_3$) improved the RF to 31.55 (% OOIP).
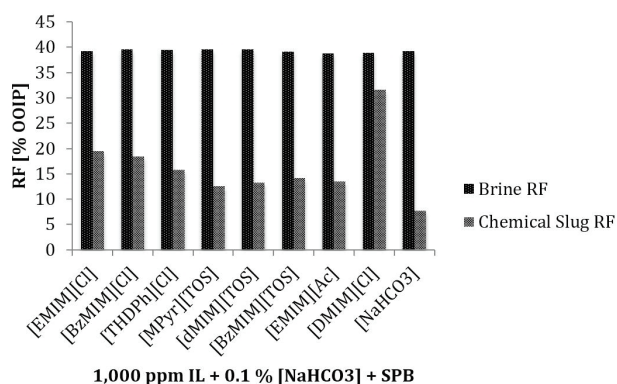

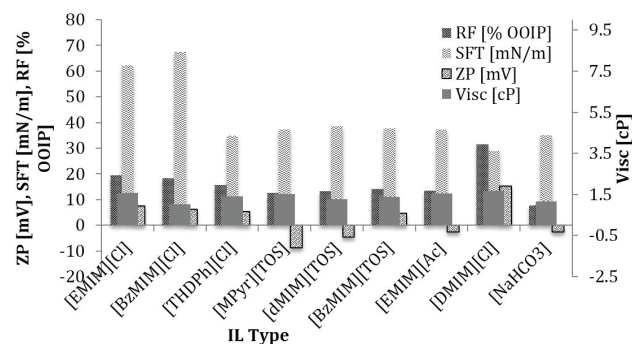**Figure 4.** The effect of NaHCO$_3$ on the efficiency of IL

Figure 5. The properties of NaHCO$_3$/IL mixtures

4.3 Effect of Chemical Slug Size on the Additional RF

1,000 (ppm) of [DMIM][Cl] + 0.1 wt. % NaHCO$_3$ + SPB chemical mixture was selected for studying the influence of altering the Slug Size (SS) on the additional RF. Three slug sizes of 0.5 PV (18.07 % OOIP), 1 PV (31.55 % OOIP), and 2 PVs (42.13 % OOIP) were investigated, as

reported in Fig. 6. Obviously, the larger the SS, the better the RF. It is apparent from our study that the combination of IL and alkali is better than injecting either of them alone. It was found, from the literature, that the 0.7 PV mixture of surfactant, NaOH, and Na_2CO_3 slug ended with better RF (17.3 % OOIP) than introducing just NaOH or Na_2CO_3 slug (2 % OOIP).[34] This result confirms the importance of injecting IL and alkali as a mixture.
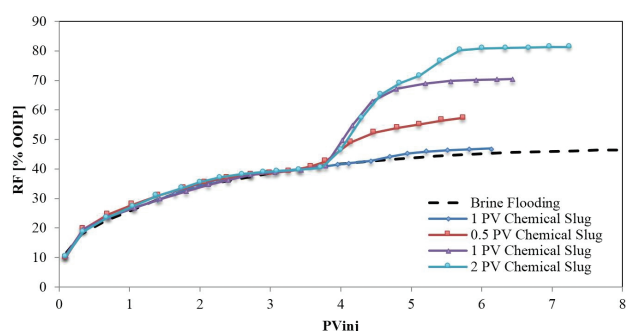

Figure 6. Slug size performance on the extra RF

5. Conclusions

Chemical flooding is a commonly used technique for EOR. The revealed enhancements in additional RF were supported by measurements of changes in zeta potential, surface tension, and viscosity values. The additional RF depends primarily on the IL type; where the weakest IL is [THTDPh][Cl] (7.87 % OOIP), and the most efficient IL is [EMIM][Cl] (14.75 % OOIP) when the studied ILs injected with brine only. For the anion type, it is clear that the RF is better when a strong aromatic ringed IL ([BzMIM][TOS]) is employed. Additionally, it was found that [EMIM][Cl] was better than [EMIM][Ac] because of the anion type efficiency. As for the cation type, it is noticed that imidazolium-based IL is more efficient than phosphonium and pyridinium cations. Higher RF values were obtained when IL with smaller alkyl chain was introduced. Noticeably, the type of the alkyl chain; anion and cation are unquestionably crucial for the performance IL and alkali mixtures. For the injected slug size, the additional RF increased with an increase in the volume of the introduced chemical slug. The improvement in the additional RF was stronger when highly aromatic, and higher ZP ILs were injected suggesting the contribution of the mechanisms based on the aromaticity interactions and electrostatic (wettability alteration) mechanisms.

Nomenclature

AIL	Alkaline + Ionic Liquid
BV	bulk volume
Ka	absolute permeability
ppm	part per million
PV	pore volume
Vo	oil volume
SARA	saturates/aromatics/resins/asphaltenes
μ	viscosity
ρ	density
$\varnothing$	porosity

References

[1] Nilsson, S.; Lohne, A. Effect of polymer on surfactant flooding of oil reservoirs, Colloid Surf. Doi: https://doi.org/10.1016/S0927-7757(97)00140-4.

[2] Thomas, S. Enhanced Oil Recovery – An Overview, Oil Gas Sci Technol – Rev. DOI: 10.2516/ogst:2007060

[3] Gong, H.; Xin, X.; Xu, G.; Wang, Y. The dynamic interfacial tension between HPAM/C17H33COONa mixed solution and crude oil in the presence of sodium halide, Colloid Surf. A 317 522–527. https://doi.org/10.1016/j.colsurfa.2007.11.034

[4] Pei, H.; Zhang, G.; Ge, J.; Tang, M.; Zheng, Y. Comparative Effectiveness of Alkaline Flooding and Alkaline–Surfactant Flooding for Improved Heavy-Oil Recovery, Energy Fuels, DOI: 10.1021/ef300206u

[5] Yadali-Jamaloei, B. Chemical Flooding in Naturally Fractured Reservoirs: Fundamental Aspects and Field-Scale Practices. Oil Gas Sci. Technol. – Rev. IFP Energies nouvelles. https://doi.org/10.2516/ogst/2010040

[6] Schramm, L. L. "Surfactants: Fundamentals and applications in the petroleum industry," Cambridge University Press, Cambridge, UK, 2000.

[7] Lake, L. W. "Enhanced oil recovery, Chapter 9-Micellar-Polymer flooding" Upper Saddle River, NJ, 07458, Prentice-Hall Inc, 1989.

[8] Simoni L.D.; Lin Y.; Brennecke J.F.; Stadtherr M.A. Modeling Liquid−Liquid Equilibrium of Ionic Liquid Systems with NRTL, Electrolyte-NRTL, and UNIQUAC, Ind Eng Chem Res, DOI: 10.1021/ie070956j

[9] Domanska, U. Solubilities and thermophysical properties of ionic liquids. Pure Appl Chem, https://doi.org/10.1351/pac200577030543

[10] Han, D.; Row, K. H. Recent Applications of Ionic Liquids in Separation Technology, Molecules. 10.3390/molecules15042405

[11] Zhao, H.; Xia, S.; Ma, P. Review Use of Ionic Liquids as 'Green' Solvents for Extractions, J Chem Technol Biotechnol. https://doi.org/10.1002/jctb.1333

[12] Johnson K. E. What's an Ionic Liquid? Interface-Electrochem Soc,2007, 16, 38-41.

[13] Bermúdez, M.D.; Jiménez, A.E.; Sanes, J.; Carrión, F. J. Ionic liquids as advanced lubricant fluids. Molecules . 10.3390/molecules14082888

[14] José-Alberto, M-H; Jorge, A. Current knowledge and

potential applications of ionic liquids in the petroleum industry. In: Kokorin, A. (Eds) Ionic Liquids: applications and perspectives. In Tech: Croatia, 439-458. Available from: http://www.intechopen.com/books/ionic-liquidsapplications-and-perspectives/current-knowledge-and-potential-applications-of-ionic-liquids-in-the-petroleumindustry

[15] Liu, J.; Huang, P.; Feng, Q.; Lian, P.; Liang, Y.; Huang, W.; Yan, H.; Jia H. Systematic investigation of the effects of an anionic surface active ionic liquid on the interfacial tension of a water/crude oil system and its application to enhance crude oil recovery. J Dispers. Sci. Technol. https://doi.org/10.1080/01932691.2018.1527230

[16] Zhou, H.; Liang, Y.; Huang, P.; Liang, T.; Wu, H.; Lian, P.; Leng, X.; Jia, C.; Zhu, Y.; Jia, H. Systematic investigation of ionic liquid-type gemini surfactants and their abnormal salt effects on the interfacial tension of a water/model oil system. J Mol Liq, https://doi.org/10.1016/j.molliq.2017.11.004

[17] Pillai, P.; Kumar, A.; Mandal A. Mechanistic studies of enhanced oil recovery by imidazolium-based ionic liquids as novel surfactants. J Ind. Eng. Chem. https://doi.org/10.1016/j.jiec.2018.02.024

[18] Manshad, A.K.; Rezaei, M.; Moradi, S.; Nowrouzi, I.; Mohammadi, A.H. Wettability alteration and interfacial tension (IFT) reduction in enhanced oil recovery (EOR) process by ionic liquid flooding. J Mol Liq, https://doi.org/10.1016/j.molliq.2017.10.009

[19] Tunnish, A. Study of Ionic Liquids as Effective Solvents For Enhanced Heavy Oil Recovery, PhD Thesis, University of Regina, Regina, SK, 2017.

[20] Tunnish, A.; Shirif, E.; Henni, A. Enhanced Heavy Oil Recovery Using 1-Ethyl-3-Methyl-Imidazolium Acetate. Can J Chem Eng, https://doi.org/10.1002/cjce.22733.

[21] Fazullin, D. D.; Mavrin, G. V.; Shaikhiev, I. G. Particle Size and Zeta Potential Changes in the Disperse Phase of Water-Emulsified Waste Waters in Different Treatment Stages. Chem Tech Fuels Oils. https://doi.org/10.1007/s10553-015-0631-8

[22] Tunnish, A., Shirif, E., Henni, A. The Influence of Ionic Liquid Type, Concentration, and Slug Size on Heavy Oil Recovery Performance. BJPG, http://dx.doi.org/10.5419/bjpg2017-0002

[23] Mohsenzadeh A.; Al-Wahaibi Y.; Al-Hajri R.; Jibril B. Effects of Concentration, Salinity and Injection Scenario of Ionic Liquids Analogue in Heavy Oil Recovery Enhancement. J Petrol Sci Eng, https://doi.org/10.1016/j.petrol.2015.04.036.

[24] Lago, S.; Rodrı´guez, H.; Khoshkbarchi, M. K.; Soto, A.; Arce, A. Enhanced Oil Recovery Using The Ionic Liquid Trihexyl(Tetradecyl)Phosphonium Chloride: Phase Behaviour and Properties. RSC Advances.2012, 2(25), 9392-9397.

[25] Pereira J.F.B.; Costa R.; Foios N.; Coutinho J.A.P. Ionic Liquid Enhanced Oil Recovery in Sand-Pack Columns. Fuel, https://doi.org/10.1016/j.fuel.2014.05.055

[26] Tunnish, A.; Shirif, E.; Henni, A. Alkaline-Ionic Liquid Slug Injection for Improved Heavy Oil Recovery. Can J Chem Eng, accepted for publication 6 December 2018. https://doi.org/10.1002/cjce.23431

[27] Hazratia, N.; Beigib, A.A.M.; Abdouss, M. Demulsification of water in crude oil emulsion using long chain imidazolium ionic liquids and optimization of parameters. Fuel, https://doi.org/10.1016/j.fuel.2018.05.010

[28] Nandwania, S.K.; Malekb, N.I.; Lada, V.N.; Chakrabortya, M.; Gupta, S. Study on interfacial properties of Imidazolium ionic liquids as surfactant and their application in enhanced oil recovery. Colloids Surf A Physicochem. Eng. https://doi.org/10.1016/j.colsurfa.2016.12.037

[29] Samanta, A.; Bera, A.; Ojha, K.; Mandal, A. Comparative studies on enhanced oil recovery by alkali–surfactant and polymer flooding. J Petrol Explor Prod Technol. https://doi.org/10.1007/s13202-012-0021-2

[30] Al-Sahhaf, T.; Ahmed, A.S.; Elkamel, A. Producing ultralow interfacial tension at the oil/water interface. J Petrol Sci Technol. https://doi.org/10.1081/LFT-120003712

[31] Martin F.D.; Oxley J.C.; Lim H. Enhanced recovery of a 'J' sand crude oil with a combination of surfactant and alkaline chemicals. In: 60th Annual technical conference and exhibition of the SPE, Las Vegas, NV, SPE 14293. https://doi.org/10.2118/14293-MS

[32] Krumrine P.H.; Falcone Jr, J. S.; Campbell, T. C. Surfactant flooding 1: the effect of alkaline additives on IFT, surfactant adsorption, and recovery efficiency. SPE J. https://doi.org/10.2118/8998-PA

[33] Krumrine P.H.; Falcone Jr, J. S.Surface, polymer, and alkali interactions in chemical flooding processes. In: International symposium on geothermal chemistry, Denver, paper SPE 11778.https://doi.org/10.2118/11778-MS

[34] Liu, Q.; Dong, M.; Ma, S.; Tu, Y. Surfactant enhanced alkaline flooding for Western Canadian heavy oil recovery. Colloids and Surfaces A: Physicochem. Eng. Aspects 293. https://doi.org/10.1016/j.colsurfa.2006.07.013

About the Publisher

Bilingual Publishing Co(BPC) is an international publisher of online, open access and scholarly peer-reviewed journals covering a wide range of academic disciplines including science, technology, medicine, engineering, education and social science. Reflecting the latest research from a broad sweep of subjects, our content is accessible worldwide – both in print and online.

BPC aims to provide an academic platform for academic exchange and cultural communication that help organizations and professionals in advancing society for the betterment of mankind. BPC hopes to be indexed by well-known databases in order to expand its scope to the science community, and eventually grow to be a reputable publisher recognized by scholars and researchers around the world.

BPC adopts the Open Journal Systems, see on ojs.bilpublishing.com

About the Open Journal Systems

Open Journal Systems (OJS) is sponsored by the Public Knowledge Project Organization from Columbia University in Canada, jointly developed by PKP, the Canadian Academic Publishing Center and Canada Simon Fraser University Library. OJS can realize the office automation of periodical editing process, station build and full-text journals by network publishing. The system design is in line with international standards, and supports peer review. It is very helpful to improve the citation rate, academic level and publication quality of periodicals.

Bilingual Publishing Co. is a company registered in Singapore in 1984, whose office is at 12 Eu Tong Sen Street, #08-169, Singapore 059819, enjoying a high reputation in Southeast Asian countries, even around the world.

9 772591 758189